University of Stavanger

FACULTY OF SCIENCE AND TECHNOLOGY

MASTER'S THESIS

Study programme/specialization: Master of Science in Engineering Structures and Materials/Mechanical Systems	Spring semester, 2020 Open / ~~Confidential~~

Author: Agit Akbas

Programme coordinator: Dimitros Pavlou Supervisor(s): Torfinn Havn

Title of master's thesis: **Investigation of critical time and temperature for pitting corrosion on 316SS cladding**

Credits: 30

Keywords: pitting corrosion, CPT, marine corrosion, localized corrosion, austenitic stainless steels, polarization curves, critical pitting temperature, critical pitting time, 316L	Number of pages: 57 + supplemental material/other: 12 Stavanger, 30th June 2020

Abstract

The austenitic stainless steel 316L is a very common and low carbon stainless steel grade. 316L has great corrosion characteristics under harsh conditions such as seawater, acidic medias etc. The presence of molybdenum offers greater resistance to corrosion than lower stainless steel grades. Welded steel parts are more susceptible to corrosion due to heat-affected zones, which is why a low carbon content alloy such as 316L is often favored. 316L have been widely used in marine applications for many decades, however localized corrosion attacks such as pitting has been observed in recent years.

This report focuses on limitations and challenges of using 316L in marine applications. The objective of this report is to examine the impact of small differences in molybdenum content, and to investigate critical pitting time and temperature for stainless steel grade 316L in natural seawater. The influence of molybdenum content was studied through several experiments. Anodic cyclic potentiodynamic polarisation curves were obtained according to ASTM G61-86 with 3.56% wt of sodium chloride solution at room temperature. The materials pitting susceptibility factor and pitting resistant equivalent numbers were calculated and compared to results from cyclic potentiodynamic polarization curves. Additionally, open circuit potentials were measured frequently in natural seawater at 4, 8 and 12 °C through 120 days. The coupons were evaluated by taking pictures before and after, and by using stereo microscopy of the surfaces before and after the experiment.

The results obtained from anodic cyclic potentiodynamic polarization revealed that variations in alloying contents influence the pitting potential where the temperature has a marginally greater effect, although the repassivation potential was not heavily affected. Based on the results obtained from coupon experiments, 2.5% molybdenum content increases the corrosion resistance to an extent. Additionally general corrosion products were observed on several coupons after 120 days of exposure, and there were no significant changes in mass after the experiment. Neither of the samples revealed localized corrosion such as pitting after exposed in natural seawater for 120 days in three different temperatures.

Preface

This master thesis is a part of a two-year engineering master course, written at University of Stavanger in spring 2020. The thesis corresponds to 30 ECT and has been taken over one semester.

The reader of this report is expected to have some technological knowledge. As there was no presentation of all the features of localized corrosion, but only a short introduction to each topic.

I would like to thank my supervisors, Prof. Torfinn Havn from UiS, Ruth Herikstad and Karl Gunnar Solheim from Subsea7 for their great guidance and support during this thesis.

I would like to thank the Institute Leader Tor Henning Hemmingsen for his guidance and support, also very grateful to lend his refrigerators for the experiment.

I would like to thank the people working in the machine lab for their help using machines and equipment's, a special thanks to Jørgen Grønsund and Johan Andreas Thorkaas for their help and supplements.

I would like to thank Utsav Raj Dotel for helping me setting up ASTM-G61 experiment, and his guidance.

I also want to show my gratitude to Subsea7 whom provided with 316L clad pipes and Rosenberg for cutting the clad pipe.

Finally, I would like to express my great gratitude to friends and family for their great support throughout the thesis. Especially my proud mother and fiancé Jindar Altan, thank you so much for your support.

Declaration

I declare that this master thesis project was carried out independently and in full compliance with the University of Stavanger (UiS) rules and regulations.

Stavanger, June 30, 2020

Agit Akbas

Table of Contents

List of Tables

List of Figures

Abbreviations

CRA   =   Corrosion Resistant Alloy

PRE   =   Pitting Resistant Equivalent

HAZ   =   Heat Affected Zone

CPT   =   Critical Pitting Temperature

SRB   =   Sulfate Reducing Bacteria

MIC   =   Microbially Induced Corrosion

LPR   =   Linear Polarisation Resistance

CPP   =   Cyclic Potentiodynamic Polarization

EPS   =   Extracellular polymeric substances

Chapter 1

Introduction

The worldwide production of stainless steel tops 12.5 million metric tons. In the early 1900s, production of stainless steel was as low as zero when the first experiments were carried out to add chromium to mild steel(9). Alloy 316 is an austenitic chromium-nickel stainless steel consisting about 2-3% molybdenum. The alloy is designed to provide increased resistance to pitting and crevice due to its molybdenum content in systems containing chlorides(10). Based on their composition, one may distinguish between diverse types of stainless steel. Such as ferritic, austenitic, and ferritic-austenitic steels. Likewise structural differences express differences in corrosion behavior, and even differences in weldability, capacity to harden, and magnetic properties.

Due to the relatively high cost of corrosion-resistant materials, pipes made exclusively by solid CRA (corrosion resistant alloy) have therefore been gradually replaced in favor of the more cost-saving clad pipes. The clad layer, of typically 3-5mm is metallurgically bonded to to the carbon steel backing material by hot rolling. Clad pipes that are metallurgically bonded are made of composite plates that have been rounded and welded together in a longitudinally direction, and the pipes are then joined together by the application of a girth weld.

Offshore oil and gas exploration has increased the sensitivity of seawater as a corrosive environment during the last few decades. Seawater has a content of chloride which gives maximum corrosion rate(11). In the large oceans, clean sea water has only slight variations in composition and corrosivity. The pH value does not differ greatly from 8.1 and its salt concentration is about 3.5%, for the most part as NaCl. But it can have a different composition in harbors and other areas near to ground sea water. This may be due to river water inflow, or contaminated sewage disposal. It has been difficult to produce a synthetic sea water with the same corrosiveness as natural sea water in corrosion tests. An important reason for this is that natural seawater contains micro-organisms that are absent in synthetic seawater, and this can have a great impact in corrosion testings. Metallic structures exposed with seawater can develop growth of marine organisms. Such as barnacles,

mussels, and also algae in the presence of daylight. Generally, these growths are termed fouling, which can induce corrosion in a material. Contrarily, under certain circumstances, these growth may give rise to protection against corrosion e.g. at steel(12) .

1.1 Objective and scope

The main objective of the thesis is to investigate the limitations and challenges of using 316L in marine applications and to examine the impact of small differences in molybdenum content. The goal of the thesis is to investigate the critical time and temperature for stainless steel 316L in natural seawater. The objective is to study following:

- Classification of corrosion types

- Protection and monitoring methods

- Classification of stainless steels and the behaviour of it in natural seawater

- To demonstrate the effect of variations in molybdenum content in natural seawater by coupon testing

- To identify the critical time and temperature of pitting.

Chapter 2

Literature Review

2.1 Steels

Steel is an alloy consisting combination of iron and carbon, the concentration of carbon varies between 0.2% and 2.1%. Amount of carbon play important role in the steel classification. Although carbon exist in iron, elements such as magnesium, chromium, vanadium and tungsten can be used to alloy the steel. Carbon concentration in the steel and other elements hardens the steel by preventing the crystal lattices in the iron atom from slipping over one another. The varying quantities of alloying elements in the steel and the ways in which they occur (soluble elements, precipitation phase) influence properties in the steel such as hardness, ductility and stress concentration. Steels with high carbon content are usually less ductile and stronger. Alloys containing high carbon are recognized as cast iron due to its low melting points and pouring capabilities(13).

The physical and mechanical characteristics of steels vary due to their carbon percentage. Steels are categorized by its carbon percentage into three categories;

- Low carbon steels, with a maximum content of 0.2%C, often called soft steels with low tensile strength, high durability and excellent welding characteristics.

- Medium carbon steels, with a composition of 0.2 - 0.6%C have low tensile strength. Its hardness and soldering characteristics are moderate

- High carbon steels, are stels with composition of 0.6 - 2%C. They show a proper characteristic rather than a hard one, depending on the carbon percentage. Its tensile strength is higher than other steels. Very good hardness, but weak and brittle.

2.1.1 Stainless steels and classifications

In 1821, French metallurgist Pierre Berthier first managed to research corrosion on iron-chrome alloys. Although metallurgist of the 19th century obtained stainless steel using low
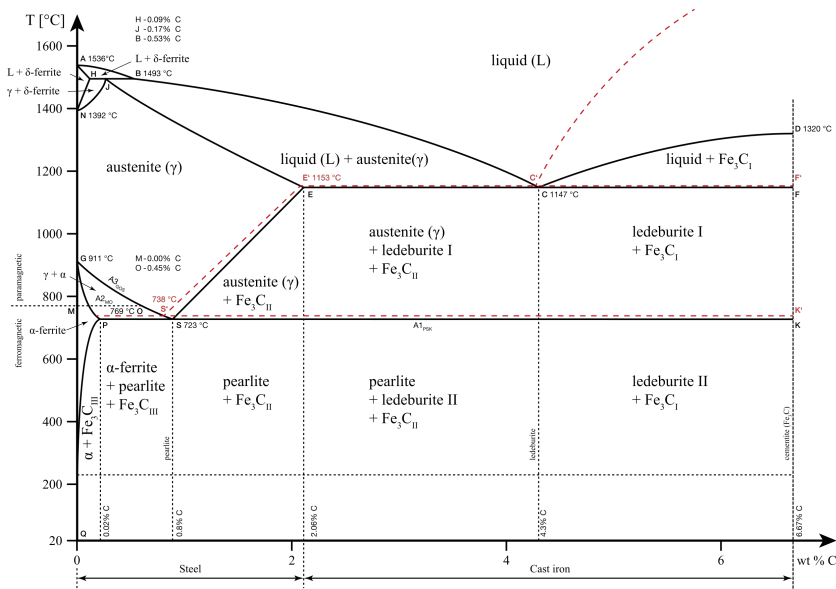
Figure 2.1: Fe-C equilibrium phase diagram, represents conditions to form different phases.

carbon and high chromium alloys, their fragility was high. German Hans Holdschhmidt found the termite reaction in 1890 generating carbonless chromium. Between 1904 and 1911, french metallurgist Léon Guillet attempted to reach stainless steel by trying different alloys. In 1908, Friedrich Krupp Germaniawerft used a chrome-nickel alloy to build a yacht called Germania. On October 17 1912, Benno Strauss and Eduard Maurer were patented for austenite stainless steel alloy on behalf of ThyssenKrupp Nirost. Similar developments took place simultaneously in USA, where Elwood Haynes applied for a martensitic stainless steel alloy and obtained a patent in 1919(14).

Stainless steels are used in almost all industries. There are different types and standards of stainless steel. In general, stainless steels contains between 10% and 25% Cr. Chromium forms on the steel surface in the steel structure and forms a layer of chromium-oxide which increases the corrosion resistance. This layer of chromium-oxide is shaped as a very thin film and has no negative impacts on the material's mechanical properties. Another element is Ni which is used as an alloying element. It improves stainless steel properties, and provides good resistance to corrosion.

There are various types of stainless steel. For instance, the austenitic microstructure of iron becomes stable when nickel is added. This crystal structure makes it a non-magnetic steel which is less brittle at low temperatures. The amount of carbon may increase hardness and strength. By adding small proportions with manganese, it is possible to maintain the austenitic structure provided with nickel at lower costs(13). Stainless steels are classified in five groups according to their crystal microstructure:

1. Austenitic stainless steels.

Alloy/Element	C %	Cr %	Ni %	Mo %	Mn %	S %	Si %
Ferritic	0.12	12-29	<2	-	1	<0.03	1
Martensitic	0.15-1	12-18	>0.75	-	<1	<0.03	<1
Austenitic	0.02-0.05	17-20	8-12	2-3	<2	<0.015	<2
Duplex	<0.03	18-26	4.5-6.5	2.5-3.5	<2	<0.02	<2
Precipitation-hardening	0.07	15.5-17.5	3-5	0.06	1.5	0.02	1.5

Table 2.1: Different chemical composition and grades of stainless steel alloys. Source: Santi- ago Arango Researchgate

2. Ferritic stainless steels

3. Martensitic stainless steels

4. Duplex stainless steels

5. Precipitation hardened stainless steels

2.1.2 Austenitic stainless steels

Generally stainless steels typically contain iron (Fe) and chromium (Cr), and the addition of appropiate amounts of austenite stabilizing elements such as nickel (Ni) and manganese (Mn) turns the stainless steel structure into austenitic stainless steel. The structure of iron alloys requires about 17 wt% Cr and 11 wt% Ni in order to achieve an austenitic structure at room temperature. However, reasonable alloying increases resistance to corrosion as the alloy composition influences the structure and properties of the passive film[15]. The key alloying element is Cr, since it defines how a passive film can form on the steel surface[16]. Additionally, in environments containing especially chloride, molybdenum (Mo) is added to enhance the pitting resistance of the alloy[17]. When the contents of Cr and Mo increase, Ni equivalents in corresponding quantities must be added[15].

2.1.3 Biofilm formation

A biofilm is a microorganism environment contained within a polymeric substance which causes significant problem for several industries.They can be described as the environment of the polymer layer they grow, created by micro-organisms[18]. Although the biofilm layer can occur in many different conditions, complex dynamics are present even in the simplest biofilm layer. Several studies have shown that biofilms accomplish their biological transition at fixed points such as beginning, maturing, preservation, and dissolution[19].

The formation of biofilms are critical step in process of pitting corrosion, as it enables cells to encounter the surface closely and create a microenvironment that is slightly different from the materials characteristics such as: pH, dissolved oxygen and organic and inorganic species[20].Bacterias in the biofilm produces extracellular polymeric substances(EPS), which helps to bind the bacterias on to each other and on to surface. However, temperature has a great impact on production of EPS, which enchances the binding capability
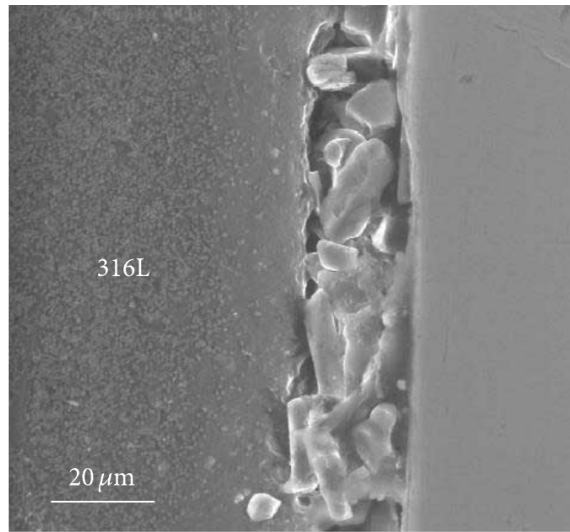
Figure 2.2: A typical SEM image representing thickness of biofilm formed on SS316 alloy.(1)

of bacterial cells(21). Therefore, EPS is critical for solid surfaces to be firmly embedded in microorganisms and for biofilm microbes to address environmental stresses, such as nutrition limitations, variations in temperatures, and solar radiations(22). Moreover, water activity can promote to survival of biofilms, which contributes to nutrient growths(23).

2.1.4 Behaviour of stainless steels in chloride containing environments

The stainless steel alloy is impacted by marine environment's corrosive nature, because it is dependent on source of oxygen to maintain its passive layer. However, at deep sea depths around 200m, seawater becomes less aggressive due to low levels of oxygen(24).

In order to choose the suitable alloy for seawater applications, pitting resistance equivalent number (PREN) measurement or CPT measurement is required to predict the resistance to localize pitting based on alloys chemical composition. In order to calculate PREN as shown in Eq. 2.1, the concentration in percent mass of alloyed elements such as Cr, Mo, W and N is used(25). PREN value greater than 40 indicates that the alloy is truly seawater resistant. According to Nickel Institute, SS316L is minimum grade for use in marine applications.

$$PREN = \%Cr + 3.3x\%Mo + 16x\%N \tag{2.1}$$

The pitting susceptibility factor (PSF) is used to evaluate the pitting corrosion resistance on various alloys if the tested alloys is in passive state and it reveals a repassivation potential at a reversed scan(26). The PSF is based on parameters obtained from cyclic polarization curves (CPP) and OCP measurements, which is calculated as shown in Eq.2.2. Typically,

Grade	Type	Cr	Mo	N	PREN
Ferritic	430	16-18	NS	>0.030	10.5-12.5
Ferritic	444	17-20	1.8-2.5	>0.030	23-28
Austenitic	304	1.5-19.5	NS	>0.11	17.5-20.8
Austenitic	316/316L	16.5-18.5	2.0-2.5	>0.11	25.3-30.7
Austenitic	4565S	24-26	4-5	0.30-0.6	42-52
Duplex	2202	22	0.4	0.2	26.5
Duplex	SAF 2304	22-24	0.1-0.6	0.05-0.20	23.1-29.2
Duplex	Ferrinox	24-26	3-4	0.2-0.3	>40^2

Table 2.2: Range of calculted PREN values for comparison. PREN value greater than 40 is considered as super duplex or super austenitic steels.

PSF rates are between 0 and 5, and values that are above or equal to 1, means that alloy is susceptible to localized corrosion(26).

$$PSF = \frac{(E_{corr} - E_{rep})}{(E_{pit} - OCP)} \tag{2.2}$$

Stainless steel family is quite extensive, their behavior in seawater depends on several factors. Seawater is often contains 3.5% NaCl. Therefore, marine environment is complex. Parameters that have effect on the corrosion behavior of stainless steels in marine environment:

- Temperature

- Movement in tidal zone

- Salinity

- Oxygen concentration

- Biological activity

2.1.5 The effect of molybdenum on stainless steels

Molybdenum (Mo) facilitates repassivation by forming in the pit bottom of an insoluble chloride salt layer(27). The formation of Mo compounds with chloride ions and results pH to increase as the amount of dissolved chloride salts decreases, thereby promoting repassivation(28). Mo enhances the passive film's solidity, especially in chlorides. Mo can emerge in several oxidation states. In the passive film for austenitic stainless steels, Mo $^{4+}$ and Mo^{6+} are present, where Mo^{4+} is selectively observable in the indigenous oxide film and is differentially present after repassivation(29). Mo's hexavalent states are MoO_3 and $MoO_4{}^{2-}$ (30).

Furthermore, a pure Mo can correspond to passivity in the passive region of an austenitic stainless steel before it experiences transpassive dissolution(31)(28). Since Mo^{6+} oxide is

fixed in state solid solution with Cr oxides and hydroxides in the passive film, Cr suppress the transpassive dissolution. It means, if Mo^{6+} oxide stability is high in chloride containing solutions, corrosion resistance to pitting increases(31)

2.2 Introduction to corrosion

Corrosion is a natural process of gradual destruction that transforms a refined metal into a more chemically stable form like oxide, hydroxide, or sulfide. It is a interdisciplinary subject, in other words, it combines elements of physics, chemistry, metallurgy, electronics and engineering. Corrosion affects material substance and is governed by energy changes(32).The metal is protected by passivity in some metal / environment systems, a naturally formed surface condition that prevents reaction. In other systems, the metal surface remains active and design must provide some form of protection; this applies in particular to low-carbon and low-alloy iron and steel, which are the most prolific, least expensive and versatile metallic materials. Corrosion occurs when mechanisms of protection have been neglected, broken down or exhausted, leaving the metal vulnerable to attack(33).
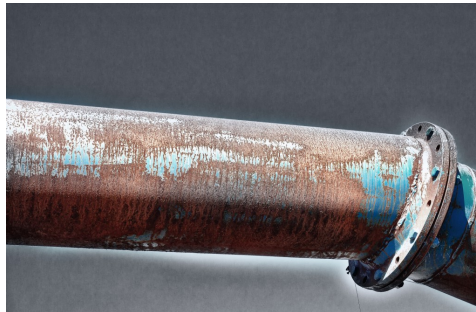
Figure 2.3: Corroded steel after several years of operation(2).

Corrosion affects many aspects of the operation of a facility, not only the availability of a industrial plant but also on the throughput and overall return on investment. Several studies in diverse economics have shown that the annual cost of corrosion amounts to 3-4 percent of the gross national product (GNP) and that the majority of corrosion problems are preventable with existing technology(34).

2.3 Mechanism of corrosion

Corrosion is the process of a material returning to natural thermodynamic state by its simplest definition. For most metallic materials, this refers to the formation of the oxides or sulfides from which they were originally taken from the earth prior to refinement into practical engineering materials. However, these changes are electrochemical reactions that follows the laws of thermodynamics. These principles demonstrate why the processes of corrosion rely on time and temperature. One of the most fundamental corrosion reactions

is the oxidation of a pure metal when it is exposed to a strong acid. The chemical reaction can be expressed as:

$$Fe + 2\,HCl \longrightarrow FeCl_2 + H_2\uparrow$$
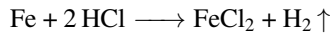
As a result of this reaction, iron gradually disappears, and hydrogen bubbles rise quickly to the surface. An electron exchange is also taking place on an electrochemical level. Such as:

$$Fe + 2\,H^+ + Cl^{2-} \longrightarrow Fe^{2+} + Cl^{2-} + H_2\uparrow$$
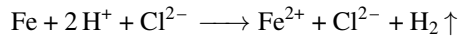
The iron has been converted to an iron ion with the release of two electrons (oxidation) which is then collected by hydrogen ions. The hydrogen was reduced by gaining electrons and hydrogen gas is formed(9). Anode and cathode definitions are among the understanding the concepts of electrochemical corrosion. The region of the corroding metal surface (i.e. at which metal dissolves into a solution) is called the anode. The cathode is the non-dissolving region of the metal surface. Reduction and oxidation reactions in the electrochemistry literature are defined as when metals lose electrons (i.e. oxidation) or gain electrons (reduction).

The "electrochemical triangle" indicates that all three factors must be present and interactive in order to cause a corrosion process. That means if one factor is removed from the triangle, the corrosion problem can be solved.
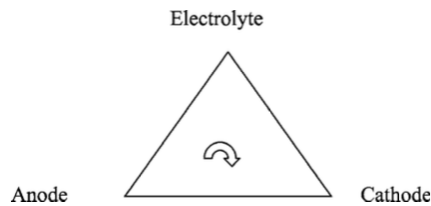
Figure 2.4: Main components of a corrosion triangle.

Corrosion can occur in fresh water, seawater, anaerobic environments, salt solutions, and alkaline or basic media. However, corrosion process occurs only if there is a dissolved oxygen present. Water solutions swiftly dissolve oxygen from the air, hence this is the source of the oxygen required in the corrosion process.

$$4\,Fe + 6\,H_2O + 3\,O_2 \longrightarrow 4\,Fe(OH)_3\downarrow$$
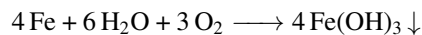
The reaction above is the most familiar corrosion type, when exposed to a moist atmosphere. It produces an insoluble reddish-brown corrosion product(4). In aerobic environments, there is presence of free oxygen, and atomic oxygen bound in such compounds as nitrate (NO_3), nitrite (NO_2), and sulphites(SO_3).
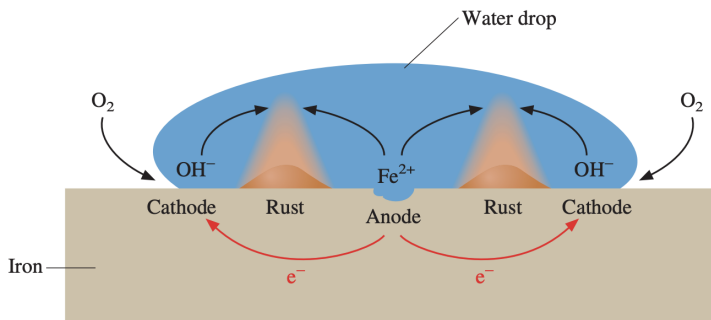
Figure 2.5: A brief sketch representing water droplet, the oxidizing iron and reduction of oxygen from air(3).

2.4 Classification of corrosion

Corrosion is conveniently classified by the forms in which it is present, and the appearance of the corroded metal is the basis for this classification. By mere visual observation, each form can be identified. The naked eye is usually sufficient, but magnification is sometimes helpful or necessary. Valuable information can often be obtained for the solution of a corrosion problem through the careful observation of the corroded tests or failed equipment(4).

2.5 Localised Corrosion

2.5.1 Uniform corrosion

Although other forms of attack must be taken into account under specific conditions, uniform attacks are one form that the metal and alloy user most frequently faces. Uniform or general corrosion is the simplest form of corrosion and equals an even rate of loss of metal over the exposed surface. It is commonly seen as metal loss because the metal part is chemically damaged or dissolved in metallic ions. Uniform metal loss usually takes precedence in high-temperature situations by its combination with other elements, rather than its oxidation to a metallic ion. Combined with oxygen, to form or scale metallic oxides, it results in material loss in its useful manufacturing form(10).

The formation of a passive film on the surface resists corrosion. The film is naturally formed when the metal is exposed to air for a certain period of time. It can also be formed faster by chemical treatment. For example, nitric acid forms that protective film when applied to austenitic stainless steel. In fact this film is a kind of corrosion, but once it's been formed it avoids further metal degradation, as long as the film remains intact(35).
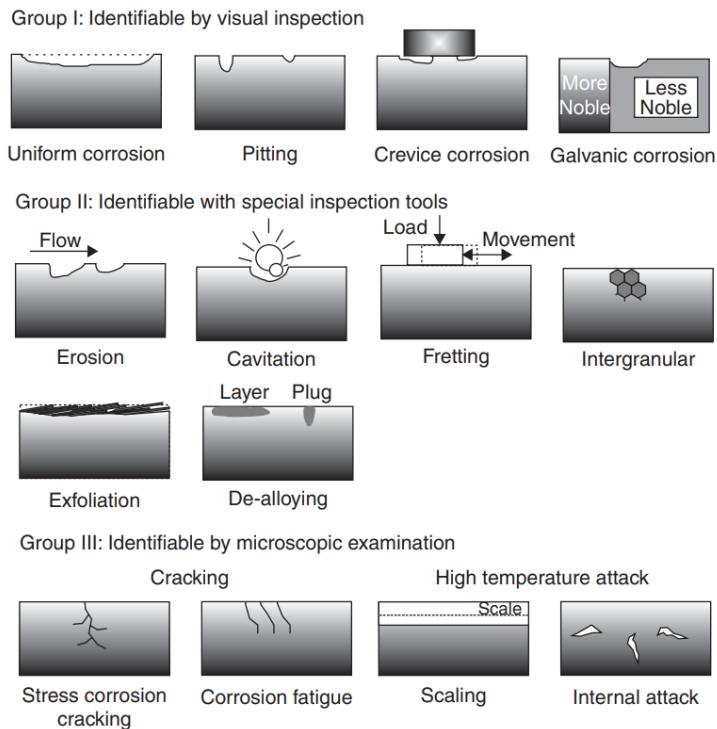
Group I: Identifiable by visual inspection

Uniform corrosion　　Pitting　　Crevice corrosion　　Galvanic corrosion

Group II: Identifiable with special inspection tools

Erosion　　Cavitation　　Fretting　　Intergranular

Exfoliation　　De-alloying

Group III: Identifiable by microscopic examination

Cracking　　　　High temperature attack

Stress corrosion cracking　　Corrosion fatigue　　Scaling　　Internal attack

Figure 2.6: Different forms of corrosion attack regrouped by ease of identification(4).

2.5.2 Pitting corrosion

Pitting corrosion is a localized form of corrosion, with attack rates in some areas being higher than in others. The main factors triggering and worsening the pitting are electrical contact between different metals or between areas of the same metal where water has varying levels of oxygen or conductive salts(35). Chlorides pose the most serious problems in several environments, such as seawater. This kind of corrosion affects many metals and their alloys (e.g. iron, nickel, copper, aluminum, steel) whereas chromium is one of the exceptions that resist pitting in aggressive environments. The limitation on pits within a large passive metal surface, which can act as a large cathode for reducing oxidants such as dissolved oxygen, results in a rapid penetration of the metal that weakens the structure and thus causes significant economic losses and safety problems(36). Pitting is considered more dangerous than uniform corrosion, since identification, prediction and design are more difficult to prevent. Only a small and narrow pit can cause an entire engineering system to fail.

In the television series called Seconds from Disaster, a spectacular catastrophe resulting from a single pit was identified. In April 1992, the sewer explosion in Guadalajara, Mexico, which caused 215 casualties, also caused a series of explosions which wounded 1500 civilians and affected 1600 buildings. Around 10:30 a.m., at least nine distinct explosions

were observed which ruptured a deep trench, almost 2 km long. At least 6 m deep and 3 m long were adjacent to the sewage network in the city and the open troughs. Many of the vehicles were crushed or crashed into them at many places in a much larger 50 m diameter craters. The loss is estimated at 75 million US dollars, according the testimony of an eyewitness(5).

Figure 2.7: Pits in a galvanized water pipe that triggered the 1992 explosion of Guadalajara: corrosion of the gas line and the resulting leakage in a sewer main(5).
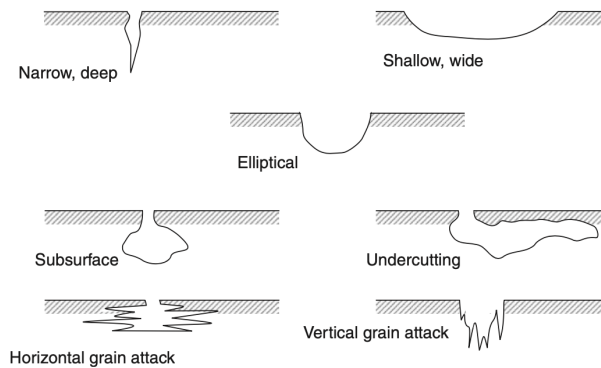
Figure 2.8: Typical shape of pitting corrosions(5).

Although the shapes of the pits differ greatly (**Fig. 2.8**)., the steel and many of the related alloys are mostly essentially saucer-like, conical and hemispherical.The factors that mostly contribute to the initiation and propagation of pitting corrosion are as follows:

- Chemical or mechanical damage localized to a protective oxide film

- Water chemistry factors which might end up causing a passive film to break, such as acidity, low concentrations of dissolved oxygen which tend to make a protective oxide film less stable and high concentrations of chloride

- Localized damage to a protective coating or a result of bad application

- Any presence of non-uniformities in for example, non-metallic inclusions in the

metal structure of the component.

Practical value of pitting corrosion relies on metal thickness and penetration rate. Significantly, penetration rate decreases if the number of pits increases. That is because the adjacent pits may exchange the applicable adjacent cathodic region, which controls the flowing corrosion current. A pit can undergo four separate steps: (1) initiation, (2) propagation, (3) termination, and (4) reinitiation.

Molybdenum is regarded as one of the major alloy elements in stainless steel and its beneficial effect in Cl-containing solutions for pitting corrosion has been widely tested over the years. However, the complexity of the molybdenum element makes it very difficult to evaluate its effects. Molybdenum content is considered to have an affect on more than one process in a pitting event. Several theories have been proposed to explain Mo's importance, it can be divided into two categories. Initially, throughout the formation of molybdates, Mo changes the polarity of the passive film and the presence of negative MoOn-ions in the external part of the film alters its purely anionic form into a cationic one, which then results in the formation of a bipolar layer. The latter promotes the transition of O^{2-} and, accordingly the formation of Cr_2O_3 and prevents Cl^- ingress to stabilize the passive film[37][38].

Critical pitting temperature (CPT)

Both temperature and the presence of chloride ions affects the pitting and crevice corrosion in marine environments[39]. Accumulation of chlorides or water evaporation can in marine conditions cause a high chloride concentration in the thin water layer covered on the steel[40]. In addition, the temperature on the steel surface depends on the functional 316L part operating temperature. Therefore, the temperature and the concentration of chloride can differ under marine environments.

Temperature is critical in terms of pitting and crevice corrosion, as the majority of the materials exhibits such attacks at a certain level, such as critical pitting temperature (CPT)[41]. Also the procedures which is outlined in ASTM G48 and G150 can be used to evalute CPT and CCT[42]. However, some researchers have proposed CPT for 316L to be 17 °C and -2 °C and lower. The difference depends on the processes and standards which is used[39]. Generally, increased temperature can have a great impact on the corrosion process in different ways. However, the rates of chemical reactions, including dissolution of metals and pit growths significantly increases with the temperature. Furthermore, there will be a rapid diffusion of species and a increase of passive film porosity[43]. Electrochemical measurements can be used to observe the effect of temperature for CRA. Also numerous authors [44][45], have shown that increased temperature allows pitting potential E_{pit} for 316L to shift towards lower potantials in NaCl solutions.

2.5.3 Microbially induced corrosion (MIC)

Microbially influenced corrosion (MIC) relates to corrosion which itself is influenced by the existence and behavior of microorganisms and/or their metabolites (products formed by their metabolism). Bacteria, fungi, and other microorganisms can play a central role in soil corrosion. Due to microbial activity, catastrophically rapid corrosion failures were

observed in the soil, and it is becoming evident that most metallic alloys are vulnerable to some type of MIC(46). Many engineers tend to be confused that the catastrophic failures of large engineering systems will result from such small species(5).It is difficult to distinguish MIC from common corrosion scenarios, according to some researchers, around 20% of all corrosion incidents are due to microorganisms(47). Biocorrosion is not limited to a single type of corrosion, rather it may cause localized attack such as crevice corrosion, pitting, erosion and galvanic corrosion and stress corrosion cracking.

One of the main criteria that affects the corrosion behaviour of stainless steel in marine environment is the microbiological activity. It has a significant influence on the potential of crevice and pitting corrosion. The macroscopic organisms such as barnacles can be attached on the surface, which may lead to crevice corrosion. The sensitivity of stainless steel in seawater is therefore unnecessary to be determined by means of a simple Na-Cl solution.Pitting corrosion is one of the most common localized attack on stainless steels. Nevertheless, if the corrosion potential rises above the pitting potential due to external factors, it may result in pitting. If the potential persists below this value, the steel will remain intact. Crevice corrosion requires a high potential in the passive region. In natural sea water, the typical pitting potential is +300 mV SCE, this is due to microbiological activities, which results oxygen reduction reaction(48).
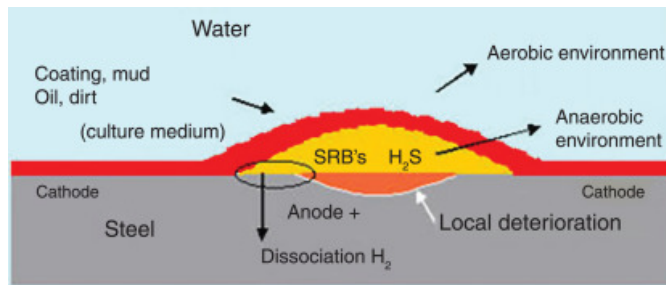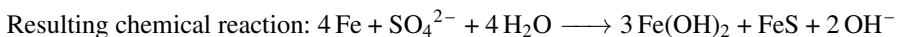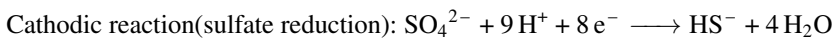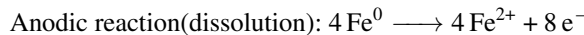

Figure 2.9: Process and formation of sulfate reducing bacteria's (SRB)

Sulfate reducing bacteria (SRB) is frequently observed in multiple oil and gas industry attributes — places as refineries and all the way into wells on an offshore oil plant. SRB can take place in any aqueous environment or soil and is a major complaint in oil and gas industries due to the inescapable nature of microorganisms and corrosive pipeline by-products. The inclusion of SRB in crude oil as microorganisms uses sulfate as an electron acceptor to produce corrosive hydrogen sulfide H_2S as their product(49). The chemical reaction of SRB is as follows:

$$\text{Anodic reaction(dissolution): } 4\,Fe^0 \longrightarrow 4\,Fe^{2+} + 8\,e^-$$

$$\text{Cathodic reaction(sulfate reduction): } SO_4{}^{2-} + 9\,H^+ + 8\,e^- \longrightarrow HS^- + 4\,H_2O$$

$$\text{Resulting chemical reaction: } 4\,Fe + SO_4{}^{2-} + 4\,H_2O \longrightarrow 3\,Fe(OH)_2 + FeS + 2\,OH^-$$

Once the hydrogen sulfide interacts with the steel, it forms specific iron sulfides and hydrogen. The hydrogen fuels the SRB, which leads to continuous developing and replication

and increasing the hydrogen sulfide levels. The activity of SRB also induces the concentration of pH and oxygen to improve results in localized attacks(49).

2.6 Corrosion monitoring methods

2.6.1 Linear polarization resistance (LPR)

Linear polarization resistance (LPR) is based on complex electrochemical concept. A small voltage (or polarization potential) is applied to an electrode in a solution and the current needed to sustain a given voltage change (typically 10 mV) is directly related to the corrosion on the electrode surface in the solution.The advantage of this method is that the estimation of corrosion rate is done instantly. Therefore, this is a much more powerful technique than either the coupon method or electrical resistance method. The disadvantage of this method is that it requires a significantly clean aqueous electrolytic environment(50).
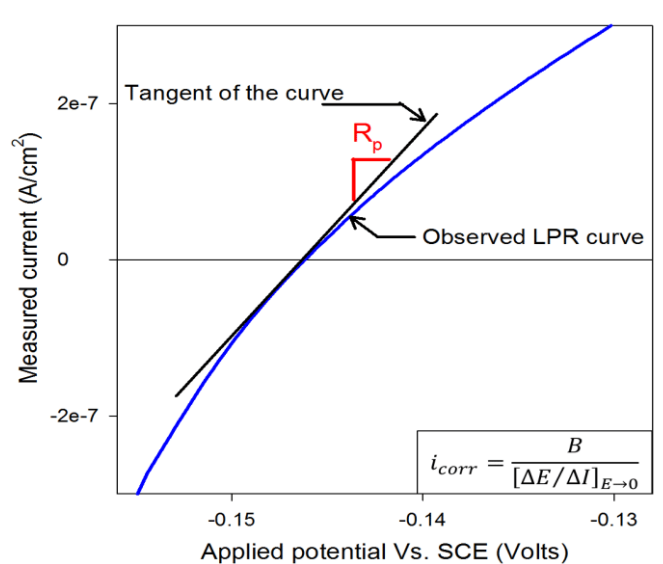

Figure 2.10: A typical LPR curve which is acquired from a specimen(6).

2.6.2 Coupon testing

Corrosion coupons are an affordable, effective approach in any system or structure to measure the corrosion rate. Nevertheless, acquiring useful data from these tests is not always as quick and easy as measuring the uniform corrosion rate or the weight loss. The most reliable results are obtained while conducting coupon testings, the size of the coupons can vary, therefore ASTM guidelines are recommended. These experiments are performed to accelerate chosen sample in aggressive conditions and high temperatures.

These tests have been successful in the classification of materials' relative resistance to localized corrosion(51). There are standard test methods which are useful in evaluating and discussing the results. Such as ASTM G4 Standard Guide for Conducting Corrosion Coupon Tests.

The most reliable results are obtained while conducting the coupon checking. Coupons can vary in size from the expected result but ASTM recommendations usually exist.

Chapter 3

Experimental procedure

The purpose of the experimental study was to investigate the limitations of AISI 316L and the impact of changes in Mo content in natural seawater. The Mo content of two experimented alloys were 2.5% and 2.0% respectively. In the first chapters, the machining procedure, coupon preparations and an overview of specimens and its configurations are represented. Three different experiments were conducted, the first experiment is coupon testing of two different alloys with different content of Mo, simulated in natural seawater in 4, 8 and 12 °C respectively. Throughout the coupon testings, OCP was frequently measured in different temperatures to relate the OCP to pitting potential. The chosen method to obtain corrosion parameters such as, pitting potential and repassivation potential was conducted in compliance with ASTM G-61.

3.1 Materials and specimens preparation

Subsea 7 supplied with two clad pipes consisting of 316L with outside diameter of 316mm and inner diameter of 266.7mm.

In order to cut the specimens to smaller pieces, the material was first circularly cut into two rings before the lathing procedure. Lathing was necessary to separate the cladding alloy from the backing steel. After the lathing, the cladding alloy was separated from the backing steel and cut into four arcs in order to cut them into dimension of 40x40mm with

Alloy	C	S	P	Si	Mn	Ni	Cr	Mo
SS316 2.0%Mo	0.021	0.001	0.037	0.460	0.920	10	17.1	2.020
SS316 2.5%Mo	0.012	0.003	0.027	0.44	0.84	10.62	16.18	2.59

Table 3.1: SS316L with different chemical compositions.

help of precise cutting tool Diskotom, as shown in **Fig. 3.1**. The chemical compositions of the alloys are listed in **Table. 3.1**.

(a) The material is circularly cut by SCK 400 before lathing.

(b) The cladding alloy is separated from the backing steel.

(c) The cladding alloy is machined carefully with Diskotom.

Figure 3.1: Removal of cladding and machining of the specimen.

Total 24 specimens of 316L containing 2.5%Mo, where 6 of the specimens contains longitudinal weld. Additionally, 15 specimens of SS316L containing 2.0%Mo with no weld, was machined in order to investigate the effect of molybdenum content.

3.2 Untreated seawater exposure

In order to investigate the limitations of SS316, untreated seawater was taken from Sola, and specimens were separately exposed for 20 and 120 days. The seawater was repeatedly changed to maintain the microorganism level. The specimens was weighted with precise weighing tool, before and after the experiment. Overview of number of coupons, given with temperature and time is represented in **Table. 3.2**.

3.3 Open circuit potential measurement

The potential of the alloy (working electrode) was measured against a calomel electrode, usually non-polarizable. The reference electrode was electrically connected to the working electrode which is put in an electrolyte container through the salt bridge. The working electrode and the reference electrode were connected with a high impedance voltmeter.

Figure 3.2: Picture of coupon experiment set up, where two coupons were contained in each container in three different refrigerators

The positive terminal of the voltmeter was connected to a reference electrode, while negative terminal was connected to working electrode. The voltmeter displayed the open circuit potential while electrodes were in the free corroding state. The experimental method for assessing the open circuit potential is briefly shown in **Figure. 3.3**.

3.4 Potentiodynamic Polarization Measurement

ASTM G61-8 is a standard method to determine the corrosion properties such as pitting potential, repassivation potential and open circuit potential. These corrosion parameters are essential to identify an alloys localized corrosion properties.

3.4.1 Preparation and procedure

The specimens was cut in small shapes with same length each. According to G61-86, a flat strip of specimen with exposing area of 1 cm^2 was required. The requirements of materials and equipment's for the experiment is enlisted below:

- A Specimen holder to mount the specimen

- Potentiostat (Gamry), such that an electrode with 1 mV is maintained. The potentiostat is required to have a potential range of -1.0 to +1.6 V and an anodic current output range of 1.0 to $10^5 \mu A$

- Electrodes, SS316L should be machined into flat (14mm) diameter disk.

- Counter electrodes, high purity platinum wire in glass. The area is required to be twice as large as the test electrode.

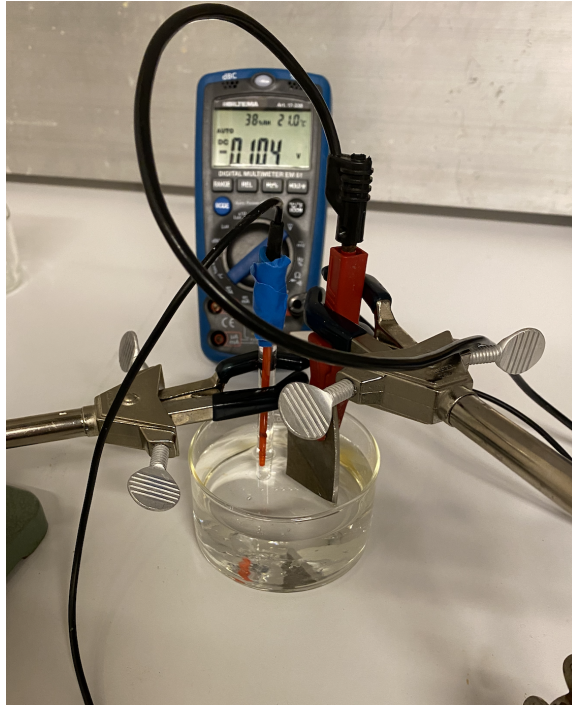- Saturated calomel electrode, in order to use it as reference electrode.

Figure 3.3: Setup of open circuit potential measurement, working electrode (the specimen) and saturated calomel electrode are put inside electrolyte.

- Distilled water

- Sodium chloride (NaCl)

- Nitrogen, to ensure that environment is oxygen-free.

The experiment was performed with 4 parallel test per material, overview of test and materials are represented in **Table. 3.3**. The procedure is as follows:

1. The test specimens was wet grinded with 240-grit paper, and thereafter wet polished with 600-grit.

2. In 920 mL of distilled water, 34g of NaCl was dissolved to produce a sodium chloride solution of 3.56% (by weight).

3. 900 mL of sodium chloride test solution was transferred to the polarization cell.

4. The experiment media solution was set to room temperature

5. Nitrogen gas was purged into the solution in order to remove oxygen

6. The working electrode (316L) and platinum auxiliary was lowered into the solution.

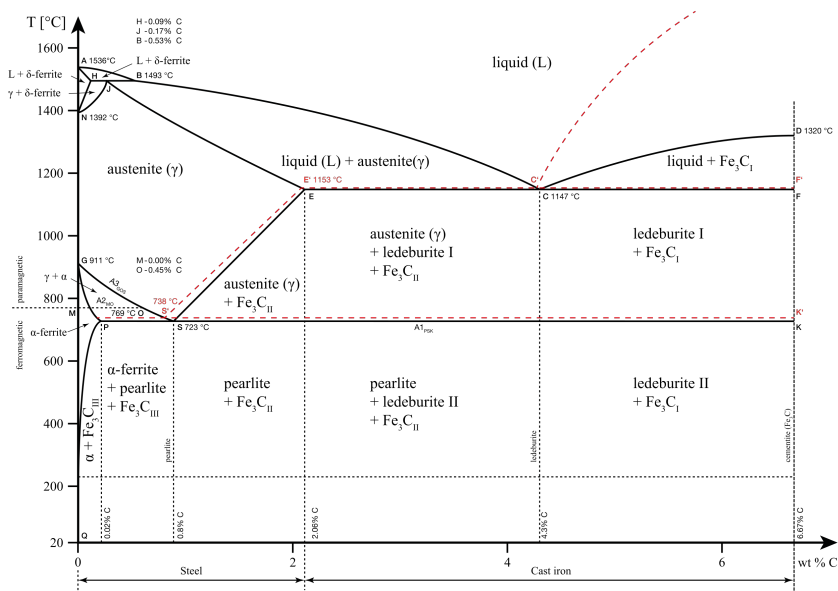7. Open circuit potential was run for 5 minutes, with help of Gamry software.

Figure 3.4: Fe-C equilibrium phase diagram, represents conditions to form different phases.

8. After specimen immersion, potential scan was started with a scan rate of 1 mV/s. The current was recorded continuously.

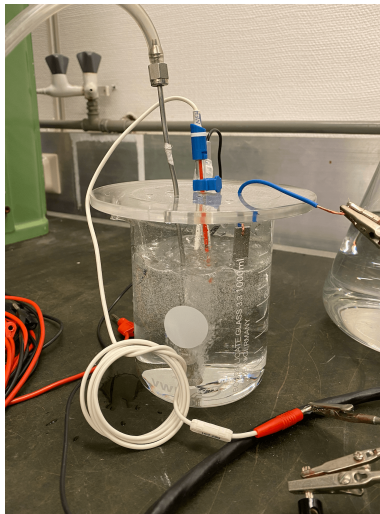9. Anodic polarization data was generated for further analysis.

Figure 3.5: Cyclic potentiodynamic polarization setup: working electrode, N_2, counter electrode and reference electrode.

Experiment type	Specimen no.	SS316 2.5%Mo	SS316 2.0%Mo
ASTM G61-86	1	PO251	PO201
	2	PO252	PO202
	3	PO253	PO203
	4	PO254	PO204

Table 3.3: Overview of parallels with specimen names.

3.4.2 Evaluation and interpretation of results

Interpretation of cyclic potentiodynamic polarization curves (CPP) can be difficult, since each curve can be different. There are critical parameters to evaluate such as, repassivation potential (E_{rep}), pitting potential (E_{pit}) and corrosion potential (E_{corr}). Nevertheless, the hysteresis which is the potential difference (E_{pit}-E_{rep})indicates the probability of pitting corrosion. The greater the difference between the current densities is the consequence of an instability of the high potential surface passivity. The large size of the hysteresis loop consequently implies more passive film breakdown as well as more uncertainty in preserving the damaged passive film(52). The path of the current density changes towards the lower current densities in the positive hysteresis. Therefore, in positive hysteresis, the slow fall in current density in the reverse scan is predictive of the complexity in surface repassivation or preventing pit growth(53).

If the current density in the forward scanning is less then reverse curve density, it indicates that there is pitting present(54).The materials resistance to localized corrosion attack is assessed against E_{corr} and E_{rep}. By analyzing which potential has the noble ideal, it is possible to envisage whether the pit is reduced or halted. The pitting potential indicates the minimum potential at which alloy tends to the pitting.

3.4.3 ASTM G61-8 deviation

The experiment had deviation from standard, as the time and equipment was limited and some methods were necessary to adjust. The changes were as follows:

- The temperature according to standard had to be around 25 °C. The distilled water was at room temperature for several days, and the temperature of the solution was around 21 °C.

- The test specimens were cleaned by ultrasonic bath and cleaned in distilled water for 5 minutes. However, according to standard, the recommendation was to wet grind and wet polish the sample with 240 grit and 600grit SiC paper, and degrease it in 5 minutes in detergent water.

- The solutions was purged with N_2 for 5 minutes, according to standard, the solutions had to be purged minimum 60 minutes to remove oxygen.

- Also the standards state that before starting the experiments, specimens had to be in the solution for at least 60 minutes. However, the experiment started right after purging of N_2 .

- The standard suggest to use a potential scan rate of 0.167, but the experiment was performed using potential scan rate of 1 mV/s.
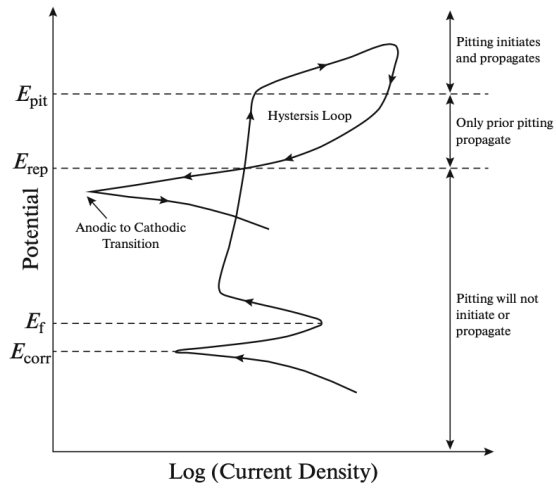

Figure 3.6: A typical CPP curve which represents important parameters.(7)

Specimen ID	Configuration	Exposure temp. (°C)	Exposure time (days)	Mass (g)	Exposure area (cm^2)
A420	No weld	4	20	37.1459	41.01
A820	No weld	8	20	44.8450	39.96
A1220	No weld	12	20	35.1712	40.84
B420	No weld	4	20	36.7302	35.9
B820	No weld	8	20	44.8448	35.02
B1220	No weld	12	20	38.1392	37.66
A840	No weld	8	110	41.7206	40.84
A840*	No weld	8	110	38.3519	40.43
A860	No weld	8	110	36.3358	39.96
A860*	No weld	8	110	45.0928	40.84
A840W	HAZ	8	110	24.7288	20.62
A860W	HAZ	8	110	27.2383	23.28
A1240	No weld	12	110	33.2970	40.84
A1240*	No weld	12	110	27.6995	41.00
A1260	No weld	12	110	33.0524	40.84
A1260*	No weld	12	110	37.1196	40.43
A1240W	HAZ	12	110	22.7379	20.42
A1260W	HAZ	12	110	36.7302	20.62
B440	No weld	4	110	40.4940	36.62
B440*	No weld	4	110	35.3216	35.84
B460	No weld	4	110	40.3222	39.42
B460*	No weld	4	110	33.4461	37.16
B840	No weld	8	110	38.7499	35.02
B840*	No weld	8	110	36.9186	36.72
B860	No weld	8	110	38.7089	36.72
B860*	No weld	8	110	38.0034	36.72
B1240	No weld	12	110	45.1047	37.66
B1240*	No weld	12	110	31.3229	36.72
B1260	No weld	12	110	39.6781	36.62
B1260*	No weld	12	110	38.0568	37.66

Table 3.2: Overview of coupons with mass and exposure area inspected before exposure.

Chapter 4

Results

4.1 Untreated seawater coupon experiment results

The coupon experiment lasted for 120 days, with seawater being changed two times a week in the first two months. However, due to COVID-19 and limited access to the laboratory, seawater was not changed for more than 60 days. The coupon test were intended to be experimented for 20, 40 and more than 60 days respectively. However, due to the laboratory shutdown, the test were carried out for 20 and 120 days. There were no pitting observed in any of the specimens. Although, some of the test samples had minor corrosion products. There where no major weight losses observed during the seawater exposure, coupons containing weld had weight loss of around 0.00005 grams, due to general corrosion. Several coupons which had no weld were also affected in form of general corrosion and had weight loss around 0.00003g after 120 days. The closer inspection of surfaces of specimens were inspected by using stereo microscopy with 5mm magnification, and no pits were observed.

(a)   (b)
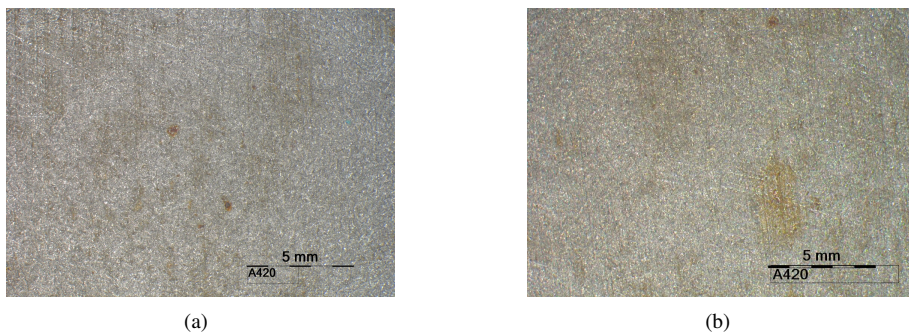
Figure 4.2: Coupon test results: (a) SS316L 2.5%Mo microscopic image of the surface before exposal (b) microscopic image after exposal

<div align="center">(a)</div>

<div align="center">(b)</div>
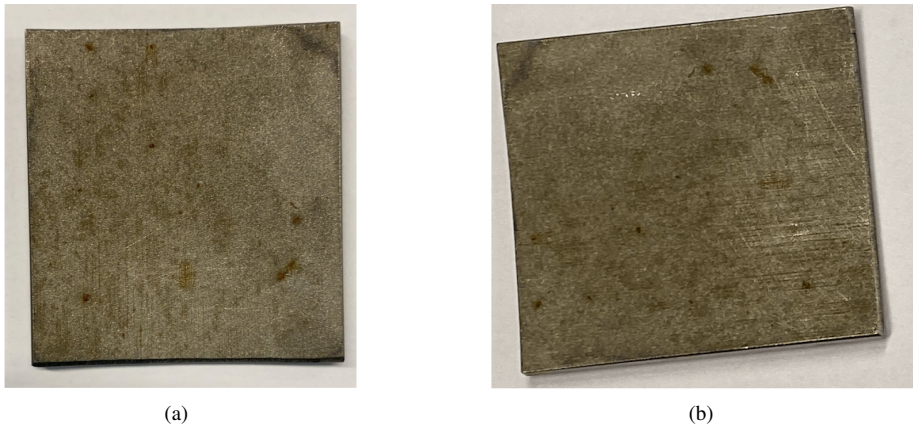
Figure 4.1: Coupon test results: (a) SS316L 2.5%Mo before exposal in seawater in 4 degrees for 120 days (b) after exposal
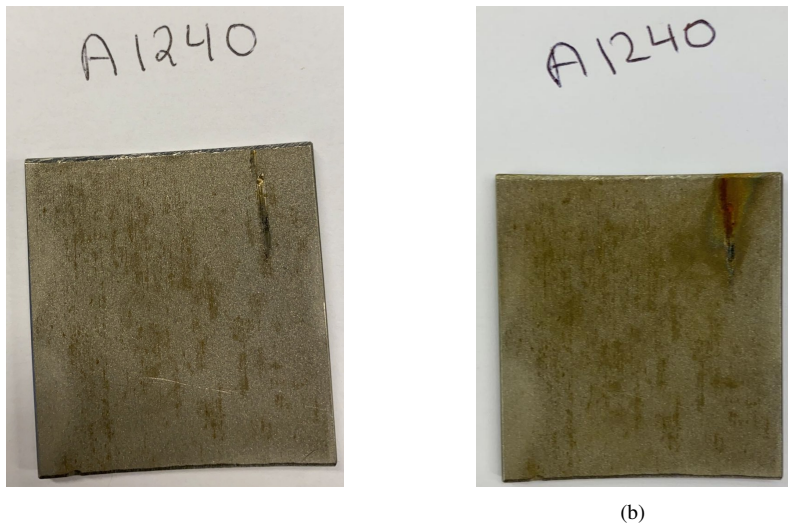

<div align="center">(b)</div>

Figure 4.4: Coupon test results: (a) SS316L 2.0%Mo before exposal in seawater in 12 degrees for 120 days (b) after exposal scratches on the surface reveals some form of corrosion
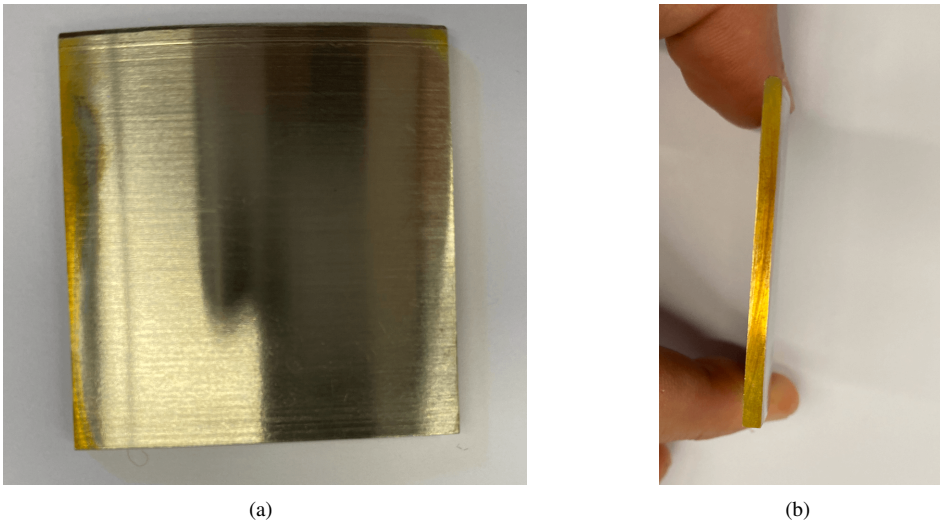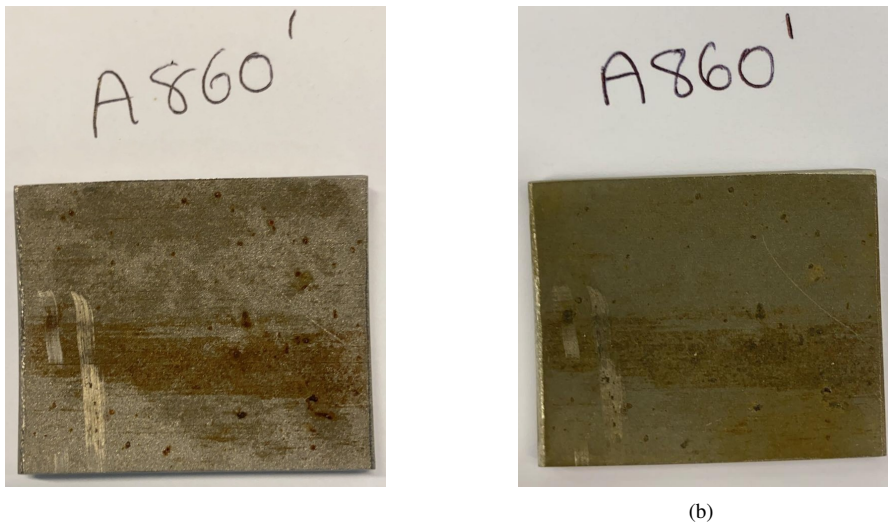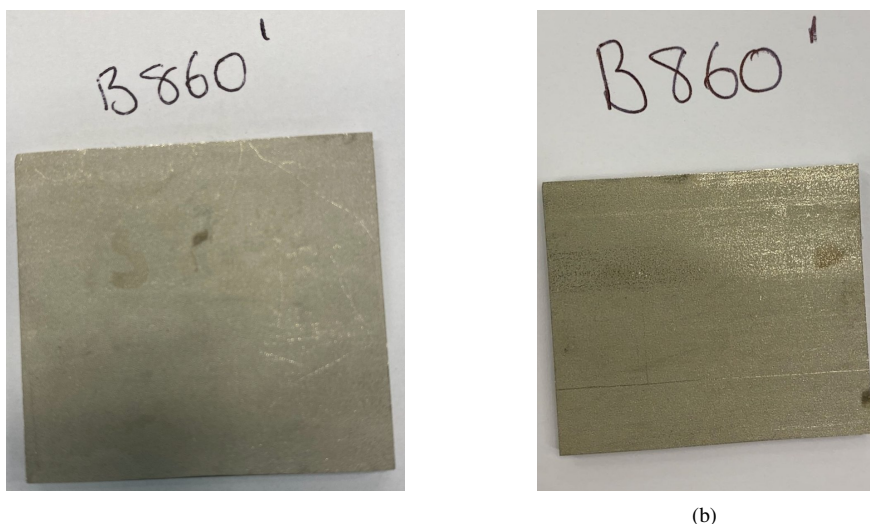
Figure 4.3: (a) Corrosion after 120 days in seawater (b) front and side of the specimen were corroded

Figure 4.7: Coupon test results: (a) SS316L 2.5%Mo before exposal in seawater in 8 degrees for 120 days (b) after exposal

(b)

Figure 4.5: Coupon test results: (a) SS316L 2.0%Mo before exposal in seawater in 8 degrees for 120 days (b) after exposal
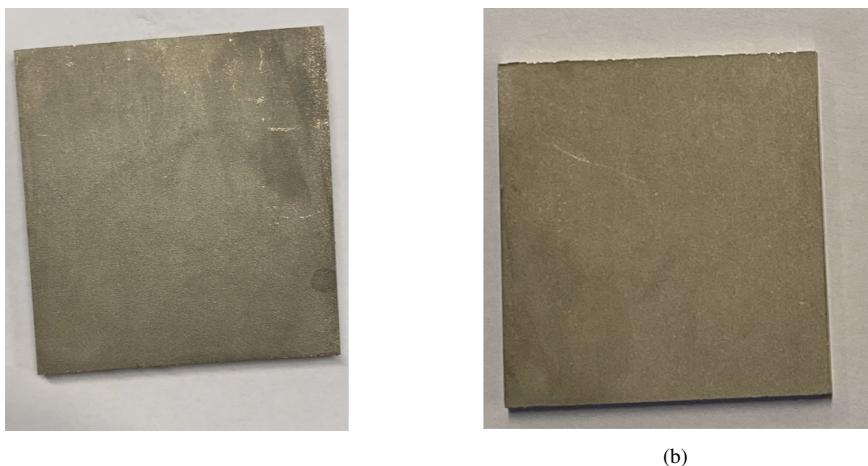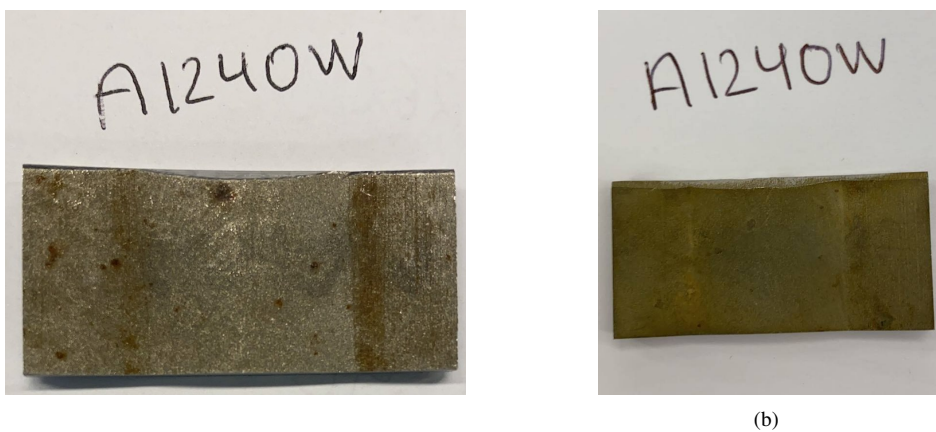

Figure 4.6: SS316L 2.5%Mo with weld in 4 degress for 120 days, sides of the specimen shows heavy corrosion.

(b)
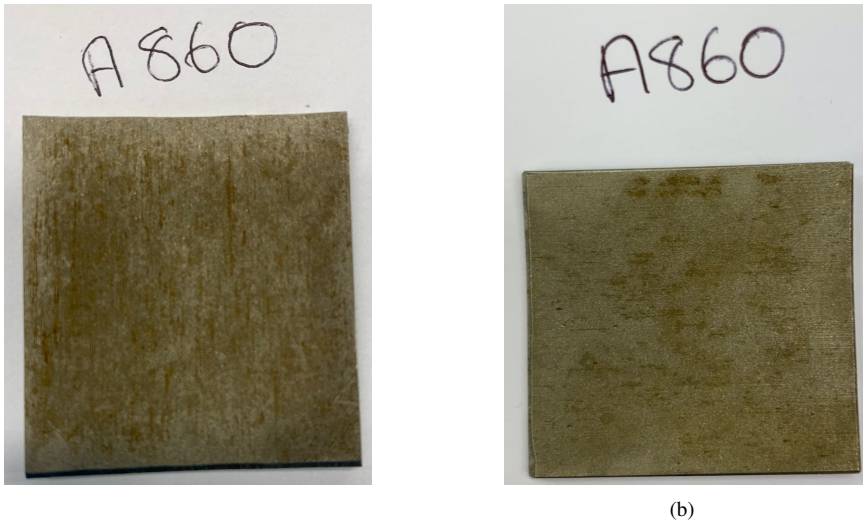
Figure 4.8: Coupon test results: (a) SS316L 2.5%Mo before exposal in seawater in 8 degrees for 120 days (b) after exposal

(b)
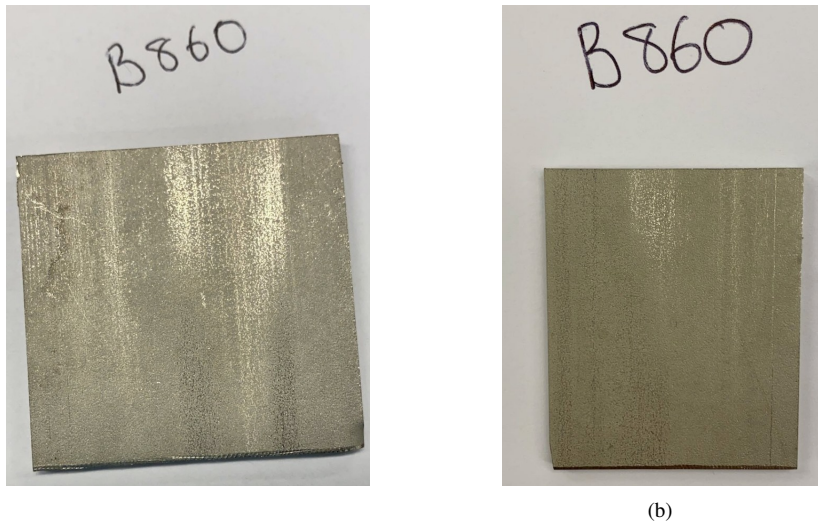
Figure 4.9: Coupon test results: (a) SS316L 2.0%Mo before exposal in seawater in 8 degrees for 120 days (a) after exposal

(b)

Figure 4.10: Coupon test results: (a) SS316L 2.0%Mo before exposal in seawater in 4 degrees for 120 days (b) after exposal

(b)

Figure 4.11: Coupon test results: (a) SS316L 2.5%Mo with weld before exposal in seawater in 12 degrees for 120 days (b) after exposal
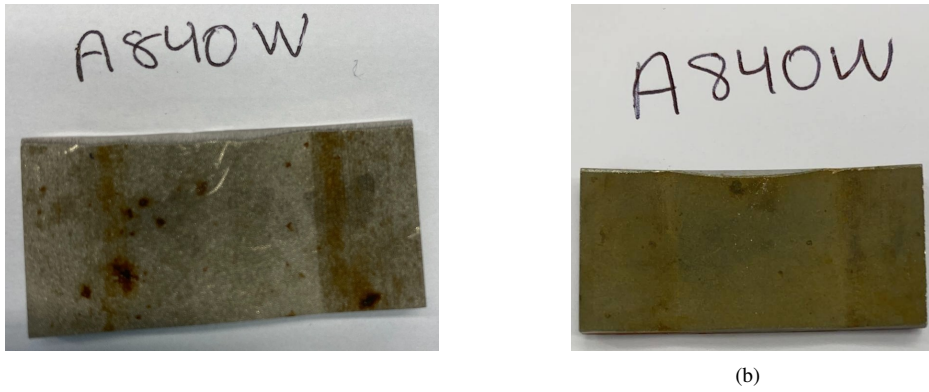
(b)

Figure 4.12: Coupon test results: (a) SS316L 2.5%Mo with weld before exposal in seawater in 8 degrees for 120 days (b) after exposal

Specimen ID	Temperature	Initial Weight	Weight after 20 days	Weight after 120 days
A420	20	37.1459	31.1459	-
A820	20	44.8450	44.8450	-
A1220	20	35.1712	35.1712	-
B420	20	36.7302	36.7302	-
B820	20	44.8448	44.8448	-
B1220	20	38.1392	38.1392	-
A840	120	41.7206	41.7206	41.7206
A840*	120	38.3519	38.3519	38.3519
A860	120	36.3358	36.3358	36.3358
A860*	120	45.0928	45.0928	45.0928
A460W	120	24.7288	24.7288	24.7279
A860W	120	27.2383	27.2383	27.2374
A1240	120	33.2970	33.2970	33.2968
A1240*	120	27.6995	27.6995	27.6695
A1260	120	33.0524	33.0524	33.0524
A1260*	120	37.1196	37.1196	37.1196
A1240W	120	22.7379	22.7379	22.7374
B420	120	36.7302	36.7302	36.7302
B440	120	40.4940	40.4940	40.4940
B440*	120	35.3216	35.3216	35.3216
B460	120	40.3222	40.3222	40.3222
B460*	120	33.4461	33.4461	33.4461
B840	120	38.7499	38.7499	38.7499
B840*	120	36.9186	36.9186	36.9186
B860	120	38.7089	38.7089	38.7089
B860*	120	38.0034	38.0034	38.0034
B1240	120	45.1047	45.1047	45.1047
B1240*	120	31.3229	31.3229	31.3229
B1260	120	39.6781	39.6781	39.6781
B1260*	120	38.0568	38.0568	38.0568

Table 4.1: Weight loss before and after the experiment.

4.2 Open Circuit Potential Measurements (OCP)

The OCP measurements were conducted for materials with 2.5%Mo and 2.0%Mo. The measurements were used to investigate the difference in pitting corrosion resistance between coupon tests, and to compare the results with anodic cyclic polarization curves with different temperatures for each parameter. The OCP test were measured in natural seawater at 4 , 8 and 12 °C.

During the measurement, the selected coupons were measured three times for 40 minutes, the median potential were obtained from three measurements. The OCP measurements

were recorded biweekly until COVID-19. There was disturbance in the measurements due to COVID-19 university shutdown, the measurements were not recorded for approximately for 9 weeks. As it can be seen from the **Table.4.2**, the potential stays stable in the first four weeks. After four weeks, potential increases by almost +80 mV SCE. The specimen were also measured after COVID-19, the potential decreased by approx. +20 mV SCE. The observations reveals that the potential increases with the temperature, and that potential between alloys with Mo content does differ to an extent.

4.3 Cyclic potentiodynamic polarization curves

Anodic CPP experiment was conducted to investigate the effect of Mo content on the relative pitting susceptibility of SS316L. The CPP curves were obtained in compliance with ASTM G-61 at room temperature. There were minor deviations between the parallels. The critical corrosion parameters obtained from CPP is represented at **Table.4.3**, with calculated PSF values according to **Eq. 2.2**. According to ASTM G-61,

The alloy with 2.5%Mo had a median E_{pit} of +367 mV/SCE, while the alloy with 2.0%Mo had a median E_{pit} of +296 mV/SCE.

Specimen ID	E_{corr} V SCE	E_{pit} V SCE	E_{rep} V SCE	OCP V SCE	PSF
PO251	-0.383	+ 0.335	+ 0.012	- 0.357	0.57
PO252	-0.264	+ 0.401	+ 0.016	- 0.109	0.54
PO253	-0.271	+ 0.288	- 0.069	- 0.186	0.42
PO254	-0.258	+ 0.443	- 0.067	- 0.174	0.31
PO201	-0.269	+ 0.323	- 0.012	- 0.252	0.71
PO202	-0.263	+ 0.286	- 0.1	- 0.262	0.30
PO203	-0.263	+ 0.292	+ 0.101	- 0.150	0.83
PO204	-0.374	+ 0.306	+ 0.101	- 0.298	0.79

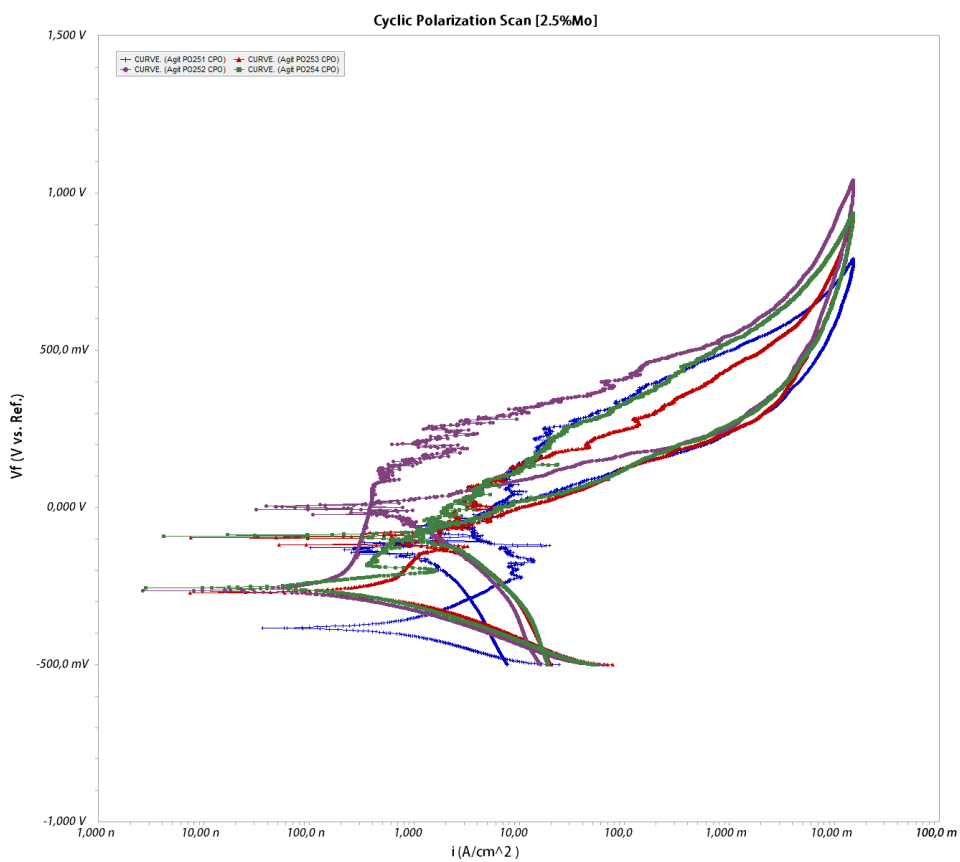**Table 4.3:** Tabulated corrosion parameters obtained from CPP.

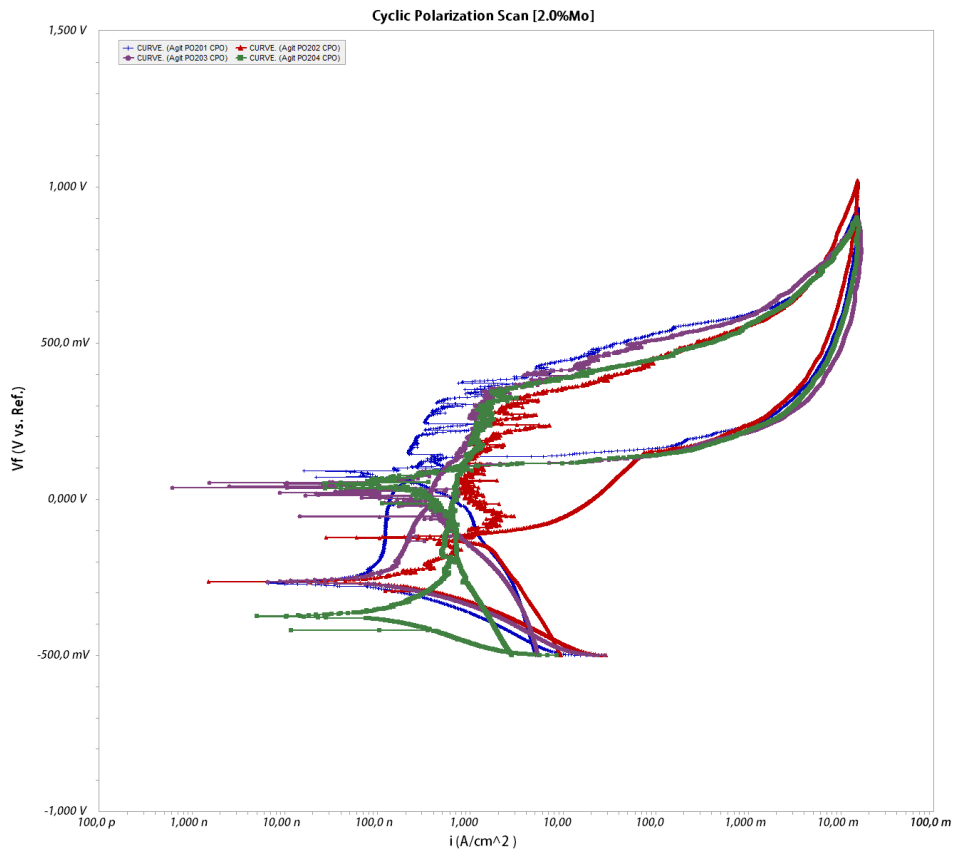**Figure 4.13:** CPP curves for SS316L 2.5%Mo with current density in x-axis and potential with respect to the reference electrode in y-axis.

Alloy 316L % Mo content	Temperature °C	Week	Open Circuit Potential (OCP) (mV)
2.5	4	1	-221
2.0	4	1	-209
2.5	8	1	-189
2.0	8	1	-147
2.5	12	1	-192
2.0	12	1	-164
2.5	4	2	-240
2.0	4	2	-232
2.5	8	2	-212
2.0	8	2	-195
2.5	12	2	-212
2.5	4	4	-201
2.0	4	4	-169
2.5	8	4	-131
2.0	8	4	-93
2.5	12	4	-122
2.0	12	4	-85
2.5	4	5	-177
2.0	4	5	-166
2.5	8	5	-142
2.0	8	5	-97
2.5	12	5	-125
2.0	12	5	-89
2.5	4	7	-191
2.0	4	7	-183
2.5	8	7	-162
2.0	8	7	-159
2.5	12	7	-121
2.0	12	7	-101
2.5	4	9	-188
2.0	4	9	-149
2.5	8	9	-133
2.0	8	9	-100
2.5	12	9	-117
2.0	12	9	-92
2.5	4	17	-160
2.0	4	17	-157
2.5	8	17	-142
2.0	8	17	-130
2.5	12	17	-124
2.0	12	17	-109

Table 4.2: Open circuit potential measurements recorded in three different temperatures.

Figure 4.14: CPP curves for SS316L 2.0%Mo with current density in x-axis and potential with respect to the reference electrode in y-axis.

Chapter 5

Discussion

5.1 Coupon testing in natural seawater

The coupon experiment lasted for 120 days, with seawater being changed biweekly in the first month. However, due to COVID-19 and limited access to the laboratory, seawater was not changed for more than 60 days, and measurements were disturbed, thus there may be deviations in the results. The OCP was measured biweekly to see if there was any biofilm formation on the specimens, thus any form of microbiological activity could risen the potential. The pH of the seawater was around 8, however since offshore sea waters are usually more polluted than sea waters closer to shore, there could be some deviations. For more than 60 days, the coupons were not inspected, and the seawater was evaporated to an extent, but some seawater was present. This has a large impact on the results, as seawater has to be changed regularly to reflect conditions at marine environments.

The coupon results did not reveal any form of pitting corrosion over 120 days. There were lids on all boxes, and there was uncertainties whether the lack of oxygen was the issue for not getting any localized corrosion. The samples that contained weld also revealed no form of pitting, but corrosion was plainly noticeable on the edges as the material's chemical composition was indeed affected by the heat-treated zone. The surface was dull after 120 days and also some form of corrosion showed on the front side.

As mentioned in chapter 2.5.2, CPT for 316L is around 17 °C. Because the experiments were carried out at low temperatures, this implies that the 316L has lower pitting developments at low temperatures. However, because some of the coupons showed general corrosion, it indicates that there was oxidation present. Additionally, OCP values were below E_{pit}, thus OCP above pitting potentials causes metastable pitting. There were no substantial changes in mass after the experiment. Although corrosion products were initiated on some coupons, it implies that if the experiment was conducted for a longer period, there would be a significant amount of mass dissolution.

From research studies done by Bastidas et al. (27), 316L has thicker passive film under wet-dry cycling immersed conditions. This means that, the corrosion resistance for 316L is higher under marine conditions since the passive film is thicker. Also another study done by Jung et al.(55) states that passive film thickness is independent on alloying content. As mentioned in chapter 2.1.3- biofilm formations are dependent on temperature, microbial environment and water activity. Since OCP observations did not reveal significant potential differences at the first 10 weeks, this may mean that there wasn't enough establishments of microorganisms. Microorganisms have many considerations, including sunlight and temperature. These factors are important to continue producing EPS, aswell as contribituion of nutrients. The experiments were done in low temperatures and inside a dark refrigerator, this may relate to the reason of the outcome. If the circumstances were realistic, then the results could have been entirely different.

An important factor considering pit propagation in immersed conditions are how corrosion products forms. The corrosion products may elevate the acidity in the electrolyte, as Fe is restricted from expanding to outer zones of the pit. The pit propagation in long term is dependent on the compositions of the corrosion products. According to Lv et.al (56), corrosion products may lower the corrosion rate over time, due to protective capabilities. The 2.5% Mo alloy was surface treated or pickled when delivered. Pickling is pre-passivation process which is done typically in acidic solutions such as sulfuric acid or hydrochloric acids to remove contaminants. It assists the formation of chromium-oxide and passive film and increase the corrosion resistance. Furthermore, this protective method can either accelerate the corrosion process or constrain it.

5.2 Cyclic Potentiodynamic Polarisation

The CPP experiment was done according to ASTM G61-68, with some configurations. As represented in chapter 4, the differences between E_{pit} and E_{rep} are of great importance when considering the effect of Mo content. A higher content of Mo means increased corrosion resistance, higher E_{pit} and E_{rep} on CPP curves.

Two materials with different Mo content were tested with four different specimens each, and some deviations were observed. The major difference between two alloys that affect the corrosion properties are content of Mo, N and Cr. Although, alloy with 2.5% Mo has a PREN value of 25.7 and the alloy with 2.0%Mo has PREN value of 24.3. There aren't notably difference in PREN values, and consequently the results do not show significant differences. However, a study done by Mudali et. al (57) and Loable et. al (16) shows that higher content of N effects the pitting potential. The alloy with 2.5%Mo has 0.024% higher N content than the alloy with 2.0%Mo, additionally the alloy with 2.5%Mo has higher content of Cr. The experiments was done in room temperature, as E_{pit} is dependent on temperature, rather than chloride concentration. The observation done by Matsch S. et. al (58) shows that temperature has great influence on E_{pit} on SS316L alloys. Since the experimented alloys doesn't have great chemical compositions, the repassivation process is almost identical, thus there is minimal difference in E_{rep} as seen in **Table 4.3.**

The OCP gathered from CPP was fluctuating and different from each samples. However,

it appears to have no effect on E_{pit} and E_{rep}. Lower OCP values causes PSF to be lower, and PSF values presented in **Table 4.3.** reveals that materials are not susceptible to pitting corrosion as PSF values are below 1. Although, the oxygen was removed from solution, thus this may cause OCP to be lower than usual.

A study done by Vallestad et. al (59) states that corrosion rates are lower under atmospheric conditions than immersed. The cathodic curves from CPP grows towards positive potentials and current densities, which emphasises the cathodic efficiency compared to atmospheric conditions. Several factors may affect the cathodic efficiency, such as sudden drop of potential and size of electrolyte under atmospheric conditions. When the cathode is immersed, the entire area operates as a cathode, whereas ohmic reduction in the electrolyte can trigger the effective cathode to be lower under atmospheric conditions. This further exemplifies consequently that under atmospheric conditions the corrosion rate is relatively lower than immersed conditions. However, the cathode areas can be smaller due to electrolytes compared to the cathodic areas under immersed conditions.

All samples represents positive hysteresis loops, which indicates that materials are susceptible to localized attacks. Nevertheless, the experiment was done with some modifications from standard, the modifications are listed in chapter 4. According to previous experiments done for SS316L, the results are approximately similar. In contrast, the calculated PSF values were below the pitting limit, as this also depends on the accuracy of the experiment. The CPP curves represented in chapter 5 shows that the alloy with 2.5%Mo exhibits a higher resistance to corrosion than the alloy with 2.0%Mo. However, during the OCP measurements, the alloy with 2.0%Mo sometimes showed higher OCP value than the 2.5%Mo alloy. This clearly indicates that when evaluating similar alloys, assessing the corrosion resistance based on CPP curves may sometimes give an incorrect evaluation.
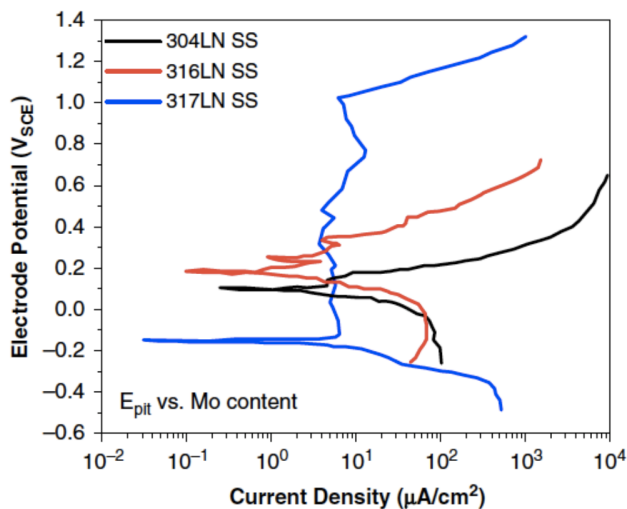
Figure 5.1: Potentiodynamic polarization curves of 316LN, 317LN and 304LN immersed in 0.01M $FeCl_3$ at room temperature with different molybdenum contents(8).

As seen in **Figure 5.1** a study done by Upadhyay et al. (8), three different stainless alloys with unique Mo content were immersed in 0.01M $FeCl_3$ at room temperature and it is observed that E_{pit} increases with Mo content. A substantial increase in E_{pit} with improved Mo content shows that higher Mo contents enhances the pitting resistance and promotes metastable pit repassivation(8). Additionally, current transient analysis was performed to investigate the effect of Mo on metastable pitting. The author Upadhyay et al. observed that 317LN revealed a higher resistance to pitting compared to 316LN.

Chapter 6

Conclusion

Based on the findings obtained from experiments, the followging conclusions are drawn:

- The effect of Mo content was studied and localized attacks such as pitting on the coupons were investigated. Based on the CPP curves it can be concluded that small changes in alloying contents affects E_{pit} to an extent, while E_{rep} is not significantly affected.

- The small difference in Mo content, does increase the corrosion resistance. Since both alloys did not reveal any pitting over 120 days, and there were differences in OCP measurements. As the alloy with 2.5%Mo had higher E_{pit} than the alloy with 2.0%Mo.

- OCP decreases with the temperature, and higher Mo content results in lower OCP.

- Based on CPP, both alloys had positive hysteresis which indicates that the alloys are susceptible to pitting corrosion.

- There were careful observations in the first months, thus it can be concluded that 316L is pitting resistant for 30 days in seawater at 4, 8 and 12 °C.

- Corrosion products were observed on specimens containing HAZ, which indicates that HAZ are weaker and is much more susceptible to general corrosion.

- According to the literature, there is still need for further understanding of 316L pitting under offshore conditions. Advancement of improved techniques and models are required to assess pitting and CPT.

- Use of 316L in seawater is valid, however it may be carefully considered.

6.1 Further work and recommendations

Further work with suggestions based on this research is described below:

- It could be interesting to perform coupon experiments on different 316L alloys containing higher Mo content.

- It is recommended to obtain CPP without O_2 to observe effect of O_2.

- Since no pitting were observed over 120 days in low temperatures, it is recommended to breakdown the passive layer to accelerate the process.

- OCP measurements should be measured every two weeks, thus there are no major changes in OCP in the short term.

- It could be interesting to perform a modified ASTM G-61, where temperature of the solution is set to 4 , 8 , and 12 °C.

- It is recommended to measure pH of the seawater to observe if the corrosion media becomes acidic over time.

- Since microorganisms activities are essential for OCP to elevate, it is recommended use seawater from offshore, since onshore sea waters are less polluted.

- During the coupon experiment, the specimens must not be on top of each other as it may result in crevice corrosion.

References

[1] "Diagnosis of the diatom community upon biofilm development on stainless steels in natural freshwater," vol. 2017, p. 13, 2017.

[2] S. Boughan. The causes and effects of corrosion in piping. [Online]. Available: http://sbmech.com/the-causes-and-effects-of-corrosion-in-piping

[3] D. Ebbing and S. D. Gammon, *General chemistry*. Cengage Learning, 2016.

[4] P. R. Roberge and P. Eng, "Corrosion engineering," *Principles and Practice*, vol. 1, 2005.

[5] P. R. Roberge, "Corrosion engineering: principles and practice," *Corrosion Engineering, Science, and Technology*, 2008.

[6] R. Pillai, S. A O Nair, J. K, B. S. Dhanya, M. Santhanam, and R. Gettu, "Enhancing the corrosion resistance of reinforced concrete structures-indian scenario and challenges ahead," 01 2015.

[7] S. Esmailzadeh, M. Aliofkhazraei, and H. Sarlak, "Interpretation of cyclic potentiodynamic polarization test results for study of corrosion behavior of metals: A review," *Protection of metals and physical chemistry of surfaces*, vol. 54, no. 5, pp. 976–989, 2018.

[8] N. Upadhyay, M. Pujar, S. S. Singh, N. G. Krishna, C. Mallika, and U. Kamachi Mudali, "Evaluation of the effect of molybdenum on the pitting corrosion behavior of austenitic stainless steels using electrochemical noise technique," *Corrosion*, vol. 73, no. 11, pp. 1320–1334, 2017.

[9] P. A. Schweitzer *et al.*, *Corrosion Engineering Handbook, -3 Volume Set*. CRC Press, 1996.

[10] ——, *Fundamentals of metallic corrosion: atmospheric and media corrosion of metals*. CRC press, 2006.

[11] E. Bardal, *Corrosion and protection*. Springer Science & Business Media, 2007.

[12] E. Mattsson, *Basic corrosion technology for scientists and engineers*. IOM Communications LTD, 2001.

[13] D. R. Jones and M. F. Ashby, *Engineering materials 2: an introduction to microstructures, processing and design*. Elsevier, 2005.

[14] H. M. Cobb, *The history of stainless steel*. ASM International, 2010.

[15] M. F. McGuire, *Stainless steels for design engineers*. Asm International, 2008.

[16] C. Loable, I. N. Viçosa, T. J. Mesquita, M. Mantel, R. P. Nogueira, G. Berthomé, E. Chauveau, and V. Roche, "Synergy between molybdenum and nitrogen on the pitting corrosion and passive film resistance of austenitic stainless steels as a ph-dependent effect," *Materials Chemistry and Physics*, vol. 186, pp. 237–245, 2017.

[17] P. Lambert, "Sustainability of metals and alloys in construction," in *Sustainability of construction materials*. Elsevier, 2016, pp. 105–128.

[18] "The biofilm matrix of pseudomonas sp. ox1 grown on phenol is mainly constituted by alginate oligosaccharides," *Carbohydrate Research*, vol. 341, no. 14, pp. 2456 – 2461, 2006.

[19] G. O'Toole, H. Kaplan, and R. Kolter, "Biofilm formation as microbial development," *Annual review of microbiology*, vol. 54, pp. 49–79, 02 2000.

[20] L. Dall'Agnol and J. Moura, "4 - sulphate-reducing bacteria (srb) and biocorrosion," in *Understanding Biocorrosion*, T. Liengen, D. Féron, R. Basséguy, and I. Beech, Eds. Oxford: Woodhead Publishing, 2014, pp. 77 – 106. [Online]. Available: http://www.sciencedirect.com/science/article/pii/B9781782421207500044

[21] D. Norwood and A. Gilmour, "The differential adherence capabilities of two listeria monocytogenes strains in monoculture and multispecies biofilms as a function of temperature," *Letters in Applied Microbiology*, vol. 33, no. 4, pp. 320–324, 2001.

[22] F. Perrot, T. Jouenne, M. Feuilloley, H. Vaudry, and G.-A. Junter, "Gel immobilization improves survival of escherichia coli under temperature stress in nutrient-poor natural water," *Water Research*, vol. 32, no. 12, pp. 3521–3526, 1998.

[23] P. R. Castro, "Capability of native yucca mountain microorganisms to corrode 1020 carbon steel," 1997.

[24] BSSA, "Selection of 316, 304 and 303 types of stainless steels for seawater applications," *Water Research*.

[25] I. . 2010, "Petroleum, petrochemical and natural gas industries—materials selection and corrosion control for oil and gas production systems," 2010.

[26] H. S. Klapper and R. B. Rebak, "Assessing the pitting corrosion resistance of oilfield nickel alloys at elevated temperatures by electrochemical methods," *Corrosion*, vol. 73, no. 6, pp. 666–673, 2017.

[27] J. Bastidas, C. Torres, E. Cano, and J. Polo, "Influence of molybdenum on passivation of polarised stainless steels in a chloride environment," *Corrosion Science*, vol. 44, no. 3, pp. 625–633, 2002.

[28] R. Willenbruch, C. Clayton, M. Oversluizen, D. Kim, and Y. Lu, "An xps and electrochemical study of the influence of molybdenum and nitrogen on the passivity of austenitic stainless steel," *Corrosion science*, vol. 31, pp. 179–190, 1990.

[29] V. Maurice, H. Peng, L. H. Klein, A. Seyeux, S. Zanna, and P. Marcus, "Effects of molybdenum on the composition and nanoscale morphology of passivated austenitic stainless steel surfaces," *Faraday discussions*, vol. 180, pp. 151–170, 2015.

[30] C.-O. Olsson and D. Landolt, "Passive films on stainless steels—chemistry, structure and growth," *Electrochimica acta*, vol. 48, no. 9, pp. 1093–1104, 2003.

[31] K. Sugimoto and Y. Sawada, "The role of molybdenum additions to austenitic stainless steels in the inhibition of pitting in acid chloride solutions," *Corrosion Science*, vol. 17, no. 5, pp. 425–445, 1977.

[32] K. Trethewey and J. Chamberlain, *Corrosion for Science and Engineering*. Longman, 1995.

[33] T. David and T. James, "Corrosion science and technology (materials science & technology)," 1997.

[34] N. Rothwell and M. Tullmin, *The corrosion monitoring handbook*. Coxmoor Pub., 2000.

[35] P. A. Schweitzer, "Encyclopedia of corrosion technology," 1998.

[36] A. Charles, "Corrosion mechanisms in theory and practice, hardback-edited by philippe marcus, marcel decker, usa, 2002. 742 pp.;," *Electrochimica Acta*, vol. 8, no. 48, p. 1081, 2003.

[37] J. Bastidas, C. Torres, E. Cano, and J. Polo, "Influence of molybdenum on passivation of polarised stainless steels in a chloride environment," *Corrosion Science*, vol. 44, no. 3, pp. 625 – 633, 2002. [Online]. Available: http://www.sciencedirect.com/science/article/pii/S0010938X01000725

[38] K. Sugimoto and Y. Sawada, "The role of molybdenum additions to austenitic stainless steels in the inhibition of pitting in acid chloride solutions," *Corrosion Science*, vol. 17, no. 5, pp. 425 – 445, 1977. [Online]. Available: http://www.sciencedirect.com/science/article/pii/0010938X77900324

[39] M. S. Thomas and A. S. Okeremi, "External pitting and crevice corrosion of 316l stainless steel instrument tubing in marine environments and proposed solution," *CORROSION 2008*, 2008.

[40] N. Johansen, "Korrosjon på aisi 316-rør," *Utfordringer og tiltak. STATOIL*, 2011.

[41] G. Frankel, "Pitting corrosion, corrosion: Fundamentals, testing, and protection, asm handbook," 2003.

[42] A. C. Tomaselli, A. Valente, F. C. Camargo *et al.*, "Super duplex saf 2507 as alternative for standard 316l in hydraulic and instrumentation tubing on topside," in *OTC Brasil*. Offshore Technology Conference, 2011.

[43] S. Mameng, R. Pettersson, and J. Jonson, "Limiting conditions for pitting corrosion of stainless steel en 1.4404 (316l) in terms of temperature, potential and chloride concentration," *Materials and Corrosion*, vol. 68, no. 3, pp. 272–283, 2017.

[44] H. Man and D. Gabe, "The study of pitting potentials for some austenitic stainless steels using a potentiodynamic technique," *Corrosion Science*, vol. 21, no. 9-10, pp. 713–721, 1981.

[45] K. Ramana, T. Anita, S. Mandal, S. Kaliappan, H. Shaikh, P. Sivaprasad, R. Dayal, and H. Khatak, "Effect of different environmental parameters on pitting behavior of aisi type 316l stainless steel: experimental studies and neural network modeling," *Materials & Design*, vol. 30, no. 9, pp. 3770–3775, 2009.

[46] P. R. Roberge, "Handbook of corrosion engineering mcgraw-hill," *New York, NY*, 2000.

[47] I. B. Beech and C. C. Gaylarde, "Recent advances in the study of biocorrosion: an overview," *Revista de microbiologia*, vol. 30, no. 3, pp. 117–190, 1999.

[48] P. E. D. I. J. Defrancq, "Corrosion of 316l stainless steel in seawater."

[49] A. S. H. Makhlouf, V. Herrera, and E. Muñoz, "Chapter 6 - corrosion and protection of the metallic structures in the petroleum industry due to corrosion and the techniques for protection," in *Handbook of Materials Failure Analysis*, A. S. H. Makhlouf and M. Aliofkhazraei, Eds. Butterworth-Heinemann, 2018, pp. 107 – 122. [Online]. Available: http://www.sciencedirect.com/science/article/pii/B9780081019283000069

[50] J. G. Speight, "Chapter 6 - corrosion monitoring and control," in *Oil and Gas Corrosion Prevention*, J. G. Speight, Ed. Boston: Gulf Professional Publishing, 2014, pp. 109 – 149. [Online]. Available: http://www.sciencedirect.com/science/article/pii/B9780128003466000065

[51] R. G. Kelly, J. R. Scully, D. Shoesmith, and R. G. Buchheit, *Electrochemical techniques in corrosion science and engineering*. CRC Press, 2002.

[52] P. J. Kinlen, D. C. Silverman, E. F. Tokas, and C. J. Hardiman, "Corrosion inhibiting compositions," Jul. 2 1996, uS Patent 5,532,025.

[53] E. McCafferty, *Introduction to corrosion science*. Springer Science & Business Media, 2010.

[54] J. A. Khamaj, "Cyclic polarization analysis of corrosion behavior of ceramic coating on 6061 al/sic p composite for marine applications," *Protection of Metals and Physical Chemistry of Surfaces*, vol. 52, no. 5, pp. 886–893, 2016.

[55] R.-H. Jung, H. Tsuchiya, and S. Fujimoto, "Growth process of passive films on

austenitic stainless steels under wet-dry cyclic condition," *ISIJ international*, vol. 52, no. 7, pp. 1356–1361, 2012.

[56] W. Lv, C. Pan, W. Su, Z. Wang, S. Liu, and C. Wang, "Atmospheric corrosion mechanism of 316 stainless steel in simulated marine atmosphere," *Corrosion Engineering, Science and Technology*, vol. 51, no. 3, pp. 155–162, 2016.

[57] U. K. Mudali and R. Dayal, "Influence of nitrogen addition on the crevice corrosion resistance of nitrogen-bearing austenitic stainless steels," *Journal of materials science*, vol. 35, no. 7, pp. 1799–1803, 2000.

[58] J. Park, S. Matsch, and H. Böhni, "Effects of temperature and chloride concentration on pit initiation and early pit growth of stainless steel," *Journal of the Electrochemical Society*, vol. 149, no. 2, p. B34, 2001.

[59] I. Vallestad, "Type aisi 316 stainless steel in chloride containing environment–effect of mo content on the corrosion properties and a pit propagation study," Master's thesis, NTNU, 2019.

Appendix
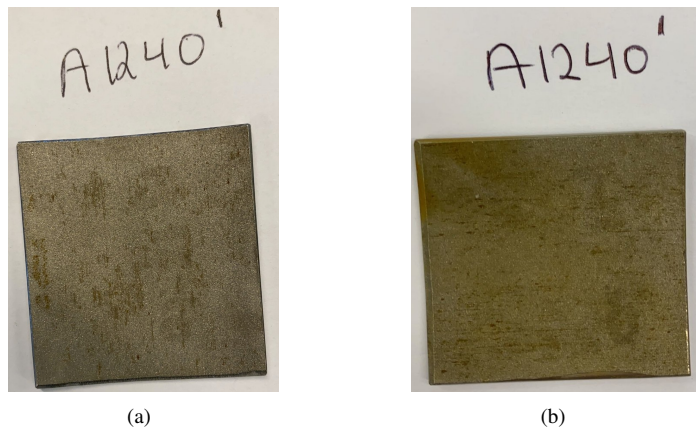
Figure 6.1: Coupon test results: (a) SS316L 2.5%Mo before exposal in seawater in 12 degrees for 120 days (b) after exposal
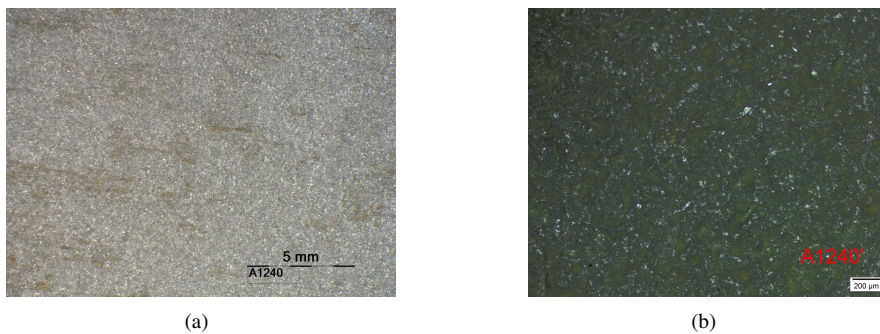
Figure 6.2: Coupon test results: (a) SS316L 2.5%Mo microscopic image of the surface before exposal in 12 °C for 120 days (b) microscopic image after exposal
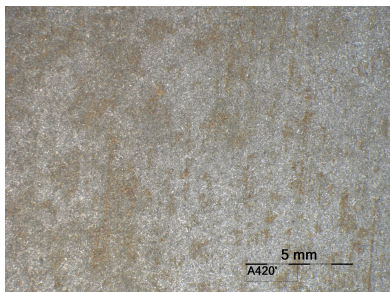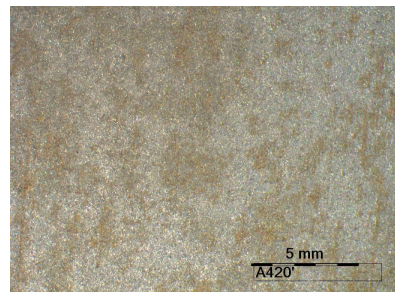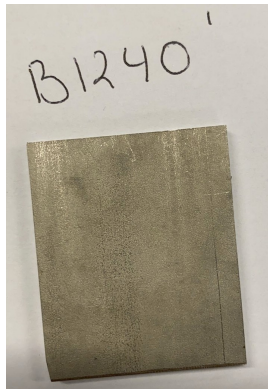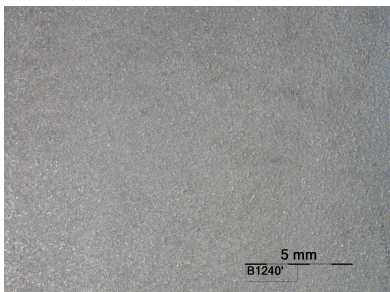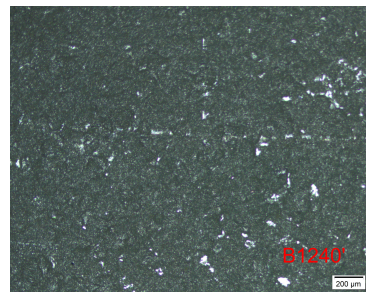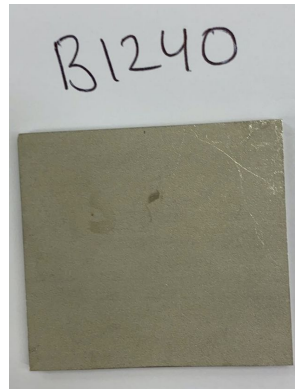
(a)   (b)
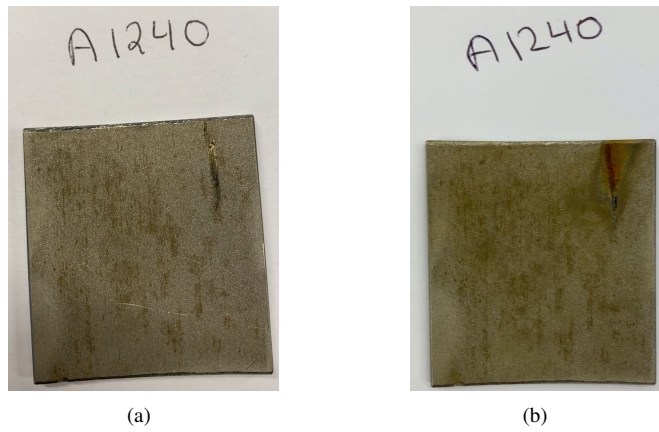
Figure 6.3: Coupon test results: (a) SS316L 2.5%Mo before exposal in seawater in 12 degrees for 120 days (b) after exposal

(a)   (b)
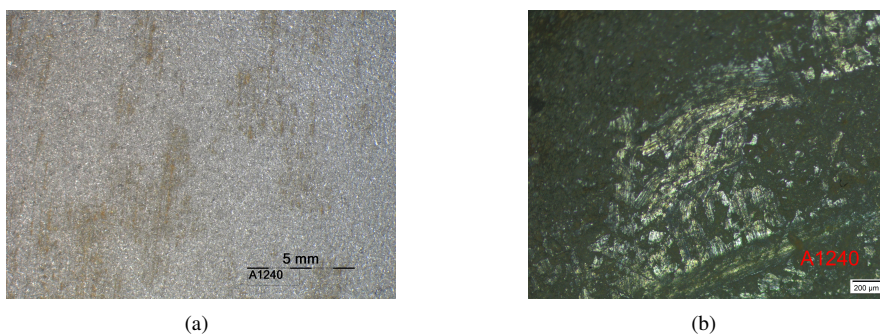
Figure 6.4: Coupon test results: (a) SS316L 2.5%Mo microscopic image of the surface before exposal in 12 °C for 120 days (b) microscopic image after exposal
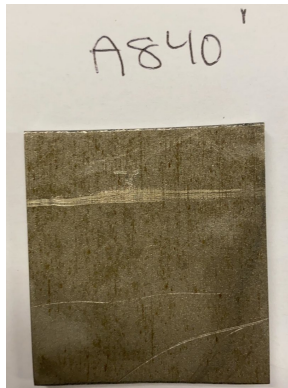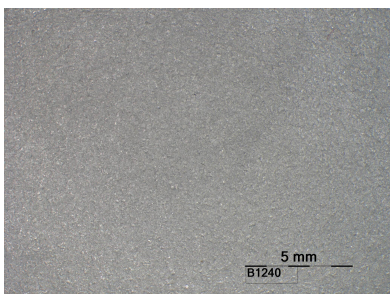
(a)
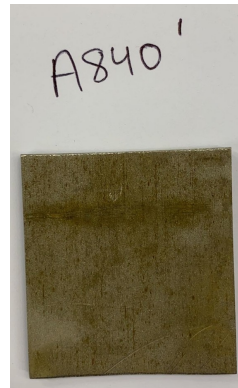
(b)

Figure 6.5: Coupon test results: (a) SS316L 2.5%Mo before exposal in seawater in 8 °C for 120 days (b) after exposal
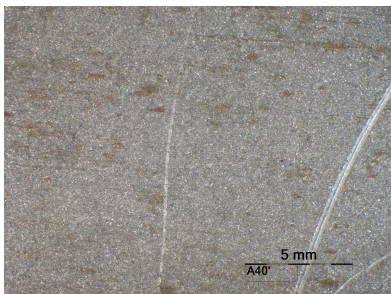
(a)
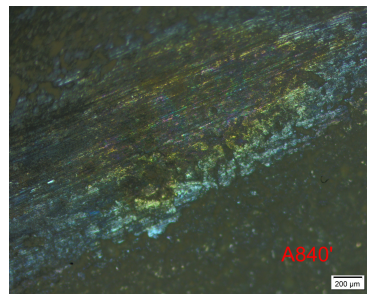
(b)

Figure 6.6: Coupon test results: (a) SS316L 2.5%Mo microscopic image of the surface before exposal in 8 °C for 120 days (b) microscopic image after exposal
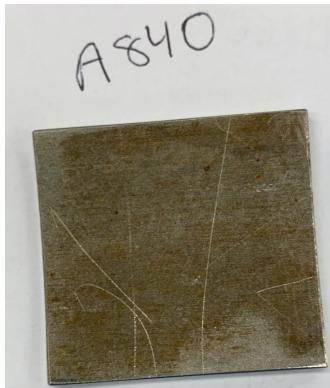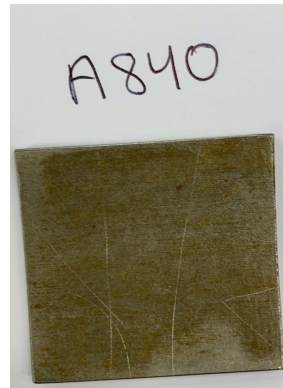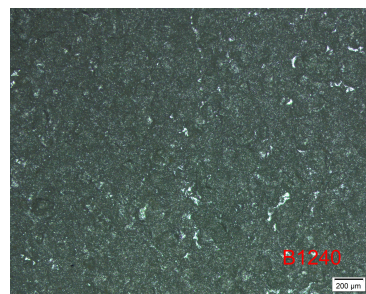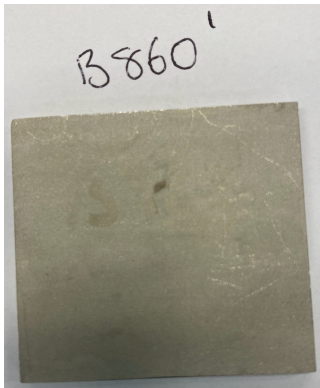
<center>(a)</center> <center>(b)</center>

Figure 6.7: Coupon test results: (a) SS316L 2.5%Mo before exposal in seawater in 8 °C for 120 days (b) after exposal
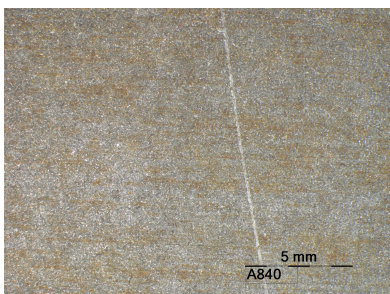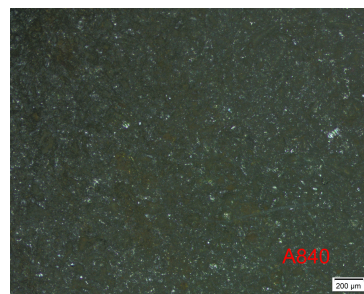
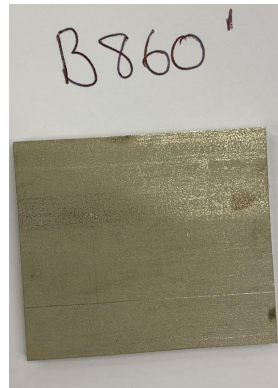<center>(a)</center> <center>(b)</center>

Figure 6.8: Coupon test results: (a) SS316L 2.5%Mo microscopic image of the surface before exposal in 8 °C for 120 days (b) microscopic image after exposal

(a)
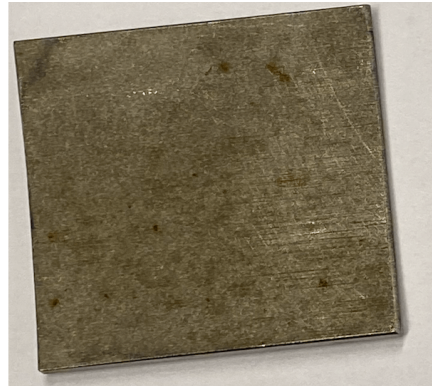
(b)

Figure 6.9: Coupon test results: (a) SS316L 2.5%Mo before exposal in seawater in 4 °C for 120 days (b) after exposal
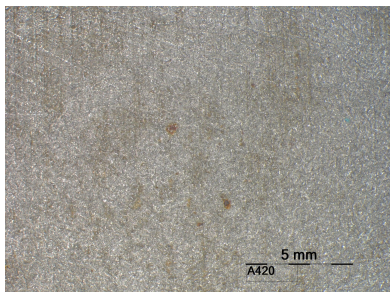
(a)
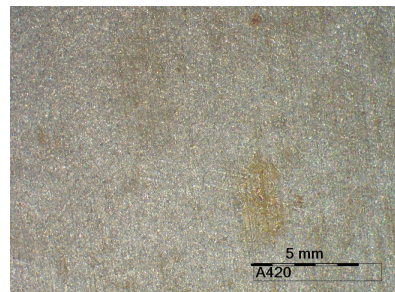
(b)

Figure 6.10: Coupon test results: (a) SS316L 2.5%Mo microscopic image of the surface before exposal in 4 °C for 120 days (b) microscopic image after exposal
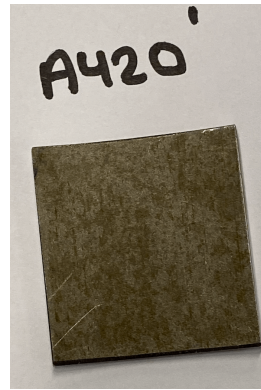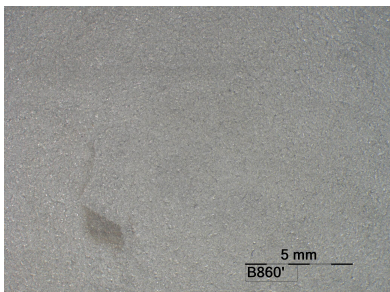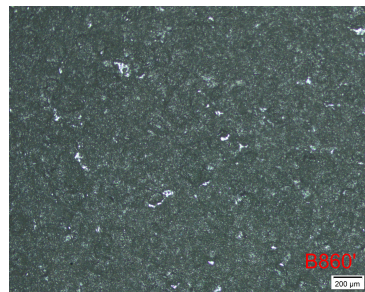
(a)   (b)

Figure 6.11: Coupon test results: (a) SS316L 2.5%Mo before exposal in seawater in 4 °C for 120 days (b) after exposal

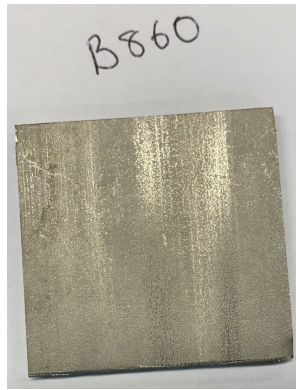(a)   (b)

Figure 6.12: Coupon test results: (a) SS316L 2.5%Mo microscopic image of the surface before exposal in 4 °C for 120 days (b) microscopic image after exposal

(a)   (b)

Figure 6.13: Coupon test results: (a) SS316L 2.0%Mo before exposal in seawater in 12 °C for 120 days (b) after exposal
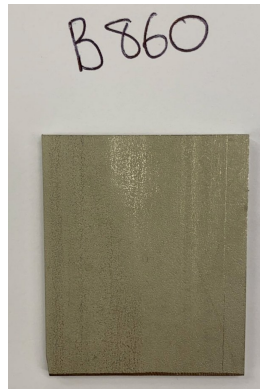

(a)   (b)

Figure 6.14: Coupon test results: (a) SS316L 2.0%Mo microscopic image of the surface before exposal in 12 °C for 120 days (b) microscopic image after exposal
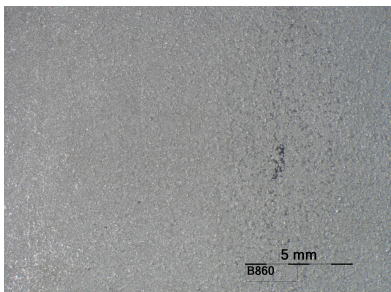
(a)

(b)

Figure 6.15: Coupon test results: (a) SS316L 2.0%Mo before exposal in seawater in 12 °C for 120 days (b) after exposal

(a)

(b)

Figure 6.16: Coupon test results: (a) SS316L 2.0%Mo microscopic image of the surface before exposal in 12 °C for 120 days (b) microscopic image after exposal
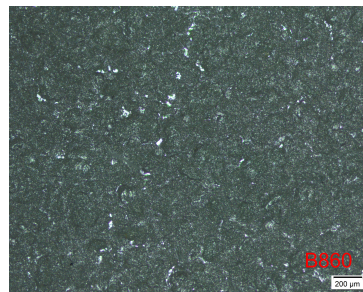
(a)   (b)

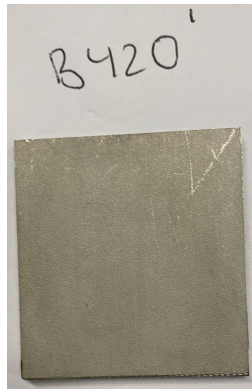**Figure 6.17:** Coupon test results: (a) SS316L 2.0%Mo before exposal in seawater in 8 °C for 120 days (b) after exposal
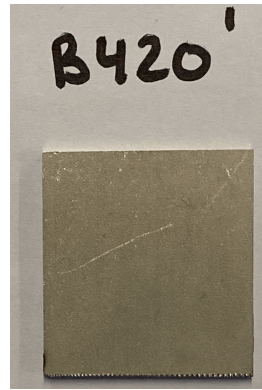

(a)   (b)

Figure 6.18: Coupon test results: (a) SS316L 2.0%Mo microscopic image of the surface before exposal in 8 °C for 120 days (b) microscopic image after exposal
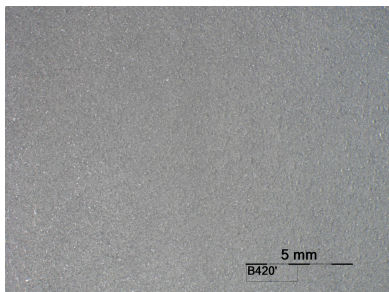
(a)   (b)

Figure 6.19: Coupon test results: (a) SS316L 2.0%Mo before exposal in seawater in 8 °C for 120 days (b) after exposal

(a)   (b)

Figure 6.20: Coupon test results: (a) SS316L 2.0%Mo microscopic image of the surface before exposal in 8 °C for 120 days (b) microscopic image after exposal
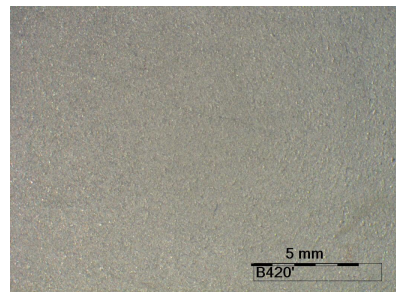
(a)   (b)

Figure 6.21: Coupon test results: (a) SS316L 2.0%Mo before exposal in seawater in 4 °C for 120 days (b) after exposal

(a)   (b)

Figure 6.22: Coupon test results: (a) SS316L 2.0%Mo microscopic image of the surface before exposal in 4 °C for 120 days (b) microscopic image after exposal
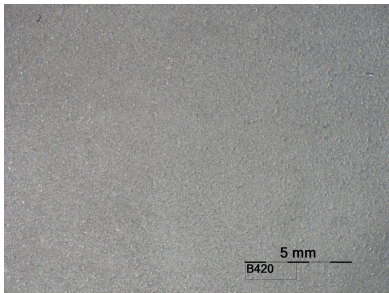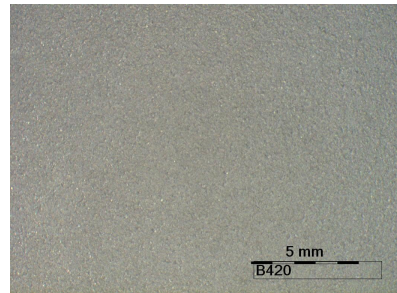
(a)

(b)

Figure 6.23: Coupon test results: (a) exposal in seawater in 4 °C for 120 days **??** after exposal

(a)

(b)

Figure 6.24: Coupon test results: (a) SS316L 2.0%Mo microscopic image of the surface before exposal in 4 °C for 120 days (b) microscopic image after exposal